LRP8 is a Receptor for Yellow Fever Virus

Miao Mei[1*], Yang Yang[2*], Zihan Zhang[3*], Yue Yin[2], Jiali Tan[1], Chao Jiang[1], Yu Gao[1], Zhaoyang Wang[4], Donghong Wang[5], Yajing Li[1], Yingyi Cong[1], Zhiyuan Zhang[6], Yousong Peng[6], Wenjie Tan[7], Jiandong Li[7], Li Li[8], Hanxue Wang[9], Ren Lang[9], Qiang He[9], Zihou Deng[8], Xiaojie Huang[10], Cao Shan[3], Yonghong Zhang[10], Gong Cheng[4], Xu Tan[1#]

1. Chinese Institute for Immunology, Chinese Institutes for Medical Research, Beijing You'an Hospital, Capital Medical University, Beijing, China
2. Shenzhen Key Laboratory of Pathogen and Immunity, National Clinical Research Center for infectious disease, State Key Discipline of Infectious Disease, Shenzhen Third People's Hospital, Second Hospital Affiliated to Southern University of Science and Technology, Shenzhen, China
3. State Key Laboratory of Virology and Biosafety, Wuhan Institute of Virology, Chinese Academy of Sciences, Wuhan 430071, China; University of the Chinese Academy of Sciences, Beijing 100039, China; Center for Biosafety Mega-Science, Wuhan Institute of Virology, Chinese Academy of Sciences, Wuhan 430071, China; Hubei Jiangxia Laboratory, Wuhan 430200, China
4. Tsinghua-Peking Center for Life Sciences, School of Medicine, Tsinghua University, Beijing; Institute of Infectious Diseases, Shenzhen Bay Laboratory, Shenzhen, China
5. School of Medicine, Tsinghua University, Beijing
6. Bioinformatics Center of College of Biology, Hunan Provincial Key Laboratory of Medical Virology, Hunan University, Changsha, China.
7. NHC Key Laboratory of Biosafety, National Institute for Viral Disease Control and Prevention, Chinese Center for Disease Control and Prevention, Beijing, 102206, China.
8. Chinese Institute for Cancer Research, Chinese Institutes for Medical Research, Capital Medical University, Beijing, China
9. Department of Hepatobiliary and Pancreatic Surgery, Beijing Chao-Yang Hospital, Capital Medical University, Beijing, China
10. Beijing You'an Hospital, Capital Medical University, Beijing, China

*: These authors contributed equally to this work

#: Correspondence should be addressed to: Xu Tan (xtan@cimrbj.ac.cn)

Abstract

Yellow fever virus (YFV), an arbovirus causing substantial human morbidity and mortality, was the first human virus discovered over a century ago. The live-attenuated 17D vaccine is among the most successful vaccines in medicine. Despite the importance of YFV, its receptor has remained unknown. Here, we performed a barcoded, genome-wide human ORF library screen and identified LRP8 (also named APOER2) as a receptor for YFV. We show that LRP8 expression specifically boosts YFV infection in cell lines by promoting entry. AAV-mediated expression of human LRP8 in mouse liver aggravates infection and pathology. LRP8 knockdown abolishes YFV infection in brain cells, primary human hepatocytes, and notably in mosquitoes. Biochemically, LRP8 directly interacts with YFV particles via the viral envelope protein. This function of LRP8 is conserved across species, particularly in mosquitoes and primates. A soluble LRP8 decoy protein can block YFV infection in vitro and in mice, providing a potential therapeutic or prophylactic strategy. Our findings provide groundwork for understanding YFV entry, tropism, and pathogenesis, and may enable development of novel therapeutics to treat YFV infection.

Introduction

Yellow fever virus (YFV), the first human virus ever discovered, is among the deadliest human pathogens and has shaped human history[1-3]. Owing to the landmark discovery in 1900[4] that mosquitoes transmit YFV and subsequent public-health efforts—particularly development and wide application of the 17D vaccine—Yellow fever (YF) is no longer considered epidemic in most countries today[5]. However, the sylvatic transmission cycle of YFV, namely transmission between non-human primates via forest mosquitoes, makes elimination highly improbable. YF remains a significant public-health concern in tropical regions of South America and Africa, with an estimated 84,000–170,000 severe cases and 29,000–60,000 deaths per year[6]. Recent outbreaks occurred in Brazil, the Democratic Republic of the Congo, Angola, Uganda, and Nigeria, with spillover cases in Asia [7]. YFV infection causes hemorrhagic fever characterized by hepatitis and jaundice. YFV infects the liver and can induce disseminated intravascular coagulation, producing hemorrhagic manifestations[8]. In late stages, the central nervous system may be affected together with multiple organ failure preceding death[8].

The attenuated 17D vaccine, developed in the 1930s, has been administered to over 500 million people, greatly reducing the burden of YFV for decades. However, vaccine production constraints during emergent outbreaks hinder rapid, comprehensive immunization[7,9]. In addition, rare serious adverse events

such as Yellow Fever Vaccine-Associated Neurotropic Disease (YEL-AND) and Yellow Fever Vaccine-Associated Viscerotropic Disease (YEL-AVD) suggest directions for improvement in next-generation vaccines[10,11]. The 17D vaccine was obtained by serial passage of the Asibi strain in mouse brain and chicken embryos (>176 passages), resulting in reduced neuro- and viscerotropism. Sequencing pinpointed 20 amino-acid differences and four additional nucleotide differences between 17D and Asibi that underlie reduced virulence[12]. Among the 20 amino-acid changes, eight reside in the envelope (E) protein, which determines tropism by engaging cellular receptors and mediating entry.[12-16].

A better understanding of the YFV life cycle would clarify tropism, pathogenesis, and the mechanism of 17D attenuation. Currently, the identity of the specific cellular receptor for YF remains unknown, hampering a molecular understanding of entry and virulence[17]. Here, we describe a genome-wide gene-overexpression screen that identifies LRP8 (also named APOER2) as a receptor for YFV. We show that LRP8 is expressed in both liver and brain, illuminating the tissue tropism of YF. Our results also highlight the effectiveness of overexpression screening in identifying viral receptors that have resisted gene-downregulation approaches such as CRISPR-Cas9 and RNAi.

Genome-wide overexpression screen to identify LRP8 as a potential YFV receptor

To uncover the long-sought YFV receptor, we applied a barcoded ORFeome library covering more than 15,000 human genes in a lentivector system driven by a CMV promoter to facilitate stable expression in mammalian cells[18,19]. We performed the screen in HEK293T cells, which have intrinsically low susceptibility to YFV. Cells were transduced with the ORFeome library at low MOI (0.1) to ensure single-ORF expression per cell. After puromycin selection, cells were infected with a recombinant YFV reporter (GFP) virus (**Fig.1a**)[20]. GFP expression enabled flow-cytometric sorting to enrich infected cells. GFP-positive and GFP-negative populations were separately processed for genomic DNA extraction, followed by PCR amplification of the barcode region adjacent to the ORF C terminus. Deep sequencing quantified the relative abundance of each ORF in the two populations. The screen was performed twice, each in triplicate. Low-density lipoprotein receptor-related protein 8 (LRP8) consistently ranked among the top candidates enriched in GFP-positive cells (**Fig.1b and Supplementary Data Set**). LRP8 (ApoER2) belongs to the low-density lipoprotein receptor (LDLR) family [21]. It is known to be expressed in the brain and plays crucial roles in neuronal development and synaptic plasticity [22,23]. Previously, LRP8 together with VLDLR, another LDLR family member,

124 was identified as an entry receptor for certain alphaviruses including Semliki
125 Forest virus, eastern equine encephalitis virus, and Sindbis virus[24]. However,
126 to the best of our knowledge, no study implicated LRP8 in flavivirus infection.
127
128 Overexpression of LRP8 dramatically enhanced infection by both 17D
129 pseudovirus, but not Zika pseudovirus, as shown by image quantification (**Fig.**
130 **1c and 1d**). Plaque assays showed that LRP8 significantly boosted infection of
131 YFV-17D live virus (**Fig. 1e**). Moreover, three major LRP8 isoforms showed
132 similar activity in promoting YF infection (**Extended Fig. 1a-1c**). In contrast,
133 overexpression of TIM1, a phosphoserine-binding protein, facilitated Zika virus
134 infection[25] and had much weaker effect on YFV infection (**Fig. 1c and 1d,**
135 **Extended Fig. 1e and 1f**). LDLR, the prototypic member of the LDLR family,
136 showed little effect on YFV infection in our ORFeome screen and validation
137 experiments (**Fig. 1b, 1c and 1d**). Because the ligand-binding domain (LBD) of
138 LRP8 mediates engagement of endogenous ligand Reelin and alphavirus
139 envelopes[12,26], we generated two LRP8 constructs: an LBD deletion (ΔLBD)
140 and an EGF-domain deletion (ΔEGF) control. Ectopic expression of
141 LRP8-ΔLBD lost the ability to promote YFV infection, whereas LRP8-ΔEGF
142 retained activity (**Extended Fig. 1a, 1b and 1d**), supporting a requirement for
143 the LBD. It is worth mentioning that LRP8-ΔLBD also has much lower protein
144 expression than those of LRP8-ΔEGF and full length protein, suggesting
145 multiple roles of LBD. We also expressed LRP8 in K562 cells, a line with very
146 low levels of endogenous LRP8[24] and showed that it also promoted YFV-17D
147 infection (**Extended Fig. 2**). Beyond the 17D vaccine strain, we tested BJ01,
148 a clinical isolate of the Angola genotype derived from a rare spillover case in
149 China[27]. YFV-BJ01 showed enhanced infection as 17D in
150 LRP8-overexpressing cells (**Fig. 1e, 1f and 1g, Extended Fig 3a, 3b**). BJ01
151 pseudovirus infection was likewise enhanced by LRP8 (**Extended Fig. 3c**).
152 Pseudotyped particles bearing E proteins from Dengue virus, Japanese
153 encephalitis virus, West Nile virus, Sepik, or Wesselsbron viruses, the latter two
154 the closest to YFV based on genome analysis[28], did not exhibit increased
155 infection in LRP8-overexpressing cells (**Fig. 1h**). Overall, LRP8 promotes YFV
156 entry in a rather specific fashion among the viruses tested.
157
158 We also generated U87-MG *LRP8* knockout (KO) cells, a glioma-origin cell line.
159 The KO was validated by FACS analysis and Western blots (**Extended Fig. 4a**
160 **and Fig. 2a**) The *LRP8*-KO cells showed profound decreases in infection by
161 YFV 17D (**Fig. 2a, 2b and 2c**) and the clinical strains BJ01 and Asibi (**Fig. 2d,**
162 **2e and Extended Fig. 4b**). Importantly, this decrease was reversed by ectopic
163 expression of sgRNA-resistant LRP8 constructs with synonymous mutations in
164 sgRNA sites, ruling out CRISPR off-target effects (**Fig. 2f, 2g and 2h,**
165 **Extended Fig. 4c, 4d and 4e**). Consistently, knockout of LRP8 had no effect

166 on Zika virus infection (**Fig. 2a, 2b and 2c**). Moreover, an antibody targeting
167 the extracellular domain of LRP8 (sc-293472) blocked YFV but not Zika virus,
168 further supporting a cell-surface receptor role (**Fig. 2i**). This antibody did not
169 block YFV infection of the LRP-KO cells, demonstrating its specificity
170 (**Extended Fig. 4f**).
171
172 **LRP8 promotes the entry of YFV**
173
174 We next examined whether LRP8 affects the entry step using 17D. Viral binding
175 to cells was measured after 90 min at 4 °C, while internalization was measured
176 after 2 h at 37 °C. Overexpression of LRP8 significantly boosted binding and
177 subsequent internalization (**Fig. 3a**). Accordingly, LRP8 knockout in U87-MG
178 cells reduced YFV binding and internalization (**Fig. 3b and 3c**). An E-targeting
179 antibody similarly inhibited binding, serving a positive control (**Fig. 3b**). An
180 imaging approach further showed that LRP8 expression promoted binding and
181 internalization of YFV virus-like particles (VLPs). Alexa Fluor 647-labeled
182 YF17D VLPs were incubated with cells at 37 °C for 30 min, washed extensively,
183 and membranes were marked with FITC-WGA. Compared to luciferase or
184 LRP8-ΔLBD, LRP8 significantly increased the number of VLPs at the
185 membrane and in the cytoplasm (**Fig. 3d and 3e**), the effect exceeded that of
186 TIM1. In contrast, VLPs bearing Zika prM/E were not significantly affected by
187 LRP8 (**Fig. 3e and 3f**). Again, the LBD was required: LRP8-ΔLBD and LDLR
188 did not promote YFV entry (**Fig. 3d and 3e**).
189
190 **LRP8 interacts with the envelope protein of YFV**
191
192 We next tested whether LRP8 interacts with the YFV envelope protein, a
193 prerequisite for a bona fide receptor. We purified Fc-tagged LRP8-LBD (LBD-Fc)
194 and performed pulldown assays. YFV envelope protein was specifically pulled
195 down with LRP8 LBD-Fc but not LDLR LBD-Fc (**Fig. 3g**). Biolayer
196 interferometry (BLI) further measured the interaction. LRP8-LBD immobilized
197 on the sensor bound purified YF17D particles with fast, strong kinetics, whereas
198 LDLR-LBD did not (**Extended Fig. 5**). Conversely, immobilized YFV particles
199 bound soluble LRP8-LBD, allowing estimation of an apparent affinity (Kd = 0.46
200 ± 0.13μM) (**Fig. 3h**). YF17D VLPs containing only E and M proteins also bound
201 LRP8-LBD with similar affinity (Kd = 0.30 ± 0.12μM) (**Fig. 3i**), together with the
202 pull-down experiment, supporting a direct E–LRP8 interaction mediated by the
203 LBD of LRP8.
204
205 **Profiling of potential receptor usages by YF17D and clinical YFV strains**
206

207 It has been demonstrated that VLDLR, another LDLR family protein highly
208 homologous to LRP8, can serve as a receptor for alphaviruses. We therefore
209 tested whether this applies to YFV. While LRP8 strongly promoted 17D, BJ01
210 and Asibi strains, VLDLR promoted infection by YF17D to a level similar to
211 LRP8 but showed a weaker effect on YFV-BJ01 or Asibi compared with LRP8
212 (**Fig. 4a, 4b and 4c**). Screening other LDLR family members revealed that, in
213 addition to LRP8 and VLDLR, only LRP4 promoted YF17D infection when
214 overexpressed (**Fig. 4a and Extended Fig. 6**). Similar to VLDLR, LRP4
215 exhibited a weaker effect on BJ01 (**Fig. 4b**). For LRP1, full-length expression
216 was not observed, likely due to its large size (>500 kDa), precluding conclusions
217 (**Extended Fig. 6**). Interestingly, mouse LRP8 and mouse VLDLR, which
218 promoted YF17D as strongly as human LRP8, supported Asibi pseudovirus and
219 BJ01 only weakly if at all (**Fig.4a and 4b**). Because YF17D was passaged in
220 mouse brain before chick embryos, adaptation to mouse LRP8 likely occurred
221 during passage.
222
223 We also tested a panel of LRP8 homologs from different species by
224 overexpression (**Fig. 4d, 4e and Extended Fig. 7 and 8**). Most homologs
225 facilitated YFV infection, indicating strong conservation from mammals to
226 mosquitoes and C. elegans. In contrast, BJ01 usage of LRP8 homologs was
227 more restricted, consistent with the shared non-conserved residues that
228 distinguish Asibi from YF17D (**Extended Fig. 9**).
229
230 **LRP8 is expressed in human liver and mediates YFV infection in primary**
231 **human hepatocytes and in a mouse model**
232
233 LRP8 is well known to be highly expressed in brain, but its expression in human
234 liver is less well characterized. Because liver is a key target organ of YFV, we
235 assessed hepatic expression of LRP8 and homologs. Immunohistochemistry
236 with two different LRP8 antibodies of human liver samples, showed clear LRP8
237 expression at levels comparable to brain (**Fig. 5a and Extended Fig. 10**). This
238 was corroborated by Western blots and single cell sequencing data of human
239 liver samples (**Fig. 5b and 5c)**. In contrast, LRP4 and VLDLR were low (**Fig.**
240 **5b and 5c)**.
241
242 Given LRP8 expression in the liver, we tested LRP8 knockdown in primary
243 human hepatocytes using siRNAs. Two siRNAs significantly reduced infection
244 of PHHs by YFV-17D and YFV-BJ01 relative to controls as measured by both
245 cellular viral RNA levels and viral titers of the media, supporting a key role for
246 LRP8 in human liver (**Fig. 5d-5i**). Accordingly, LRP8 decoy protein also blocked
247 YFV infection of PHHs (**Extended Fig. 11a**).
248

To test human LRP8 in vivo, we used Adeno-associated virus (AAV) to overexpress LRP8 in the liver of AG129 mice, which are deficient in the interferon signaling pathway and thus useful for modeling YFV-associated viscerotropic disease[8]. The overexpression levels were confirmed by Western blots of the mouse livers (**Extended Fig. 11b**). Compared with LDLR overexpression (which does not promote YFV entry), LRP8 significantly aggravated pathology after BJ01 infection (**Fig. 5j**). Survival of mice with liver-specific LRP8 expression was significantly worse than with LDLR, correlating with higher viral titers, elevated MCP-1, and increased ALT/AST/bilirubin (**Fig. 5k-5p**). Survival in the LDLR group was similar to empty-AAV controls, further supporting LRP8-mediated enhancement in vivo.

LRP8 mediates YFV 17D infection in mosquitoes

Because mosquitoes have a single LRP8/VLDLR-like gene (**Extended Fig. 7**), we used in vivo gene knockdown via injection of synthesized double-stranded RNA (dsRNA) targeting *Aedes aegypti* VLDLR in the thorax. Four dsRNAs effectively knocked down VLDLR, and correspondingly blocked infection by YF17D as measured by RT-qPCR (**Fig. 6a and 6b**). Consistent with cellular experiments, this block was specific to YFV and had no effect on Zika virus infection (**Fig. 6c and 6d**). These results, together with the overexpression data, confirm that the mosquito LRP8 homolog is a key factor mediating YFV infection in a natural host.

.

Purified Ectodomain of LRP8 protein blocks YFV infection

YFV infection of immunocompetent mice causes mortality when injected intracerebrally, a well-established model for assessing virulence. Using this model, we employed a decoy approach to test LRP8 function in mice. Purified Fc-tagged LRP8-LBD demonstrated dose-dependent, specific inhibition of YFV infection in U87-MG cells (**Fig. 6e**). C57BL/6 mice were injected intracerebrally with 17D preincubated with either purified Fc-tagged LRP8-LBD or an isotype IgG control. Mortality was significantly decreased in the LRP8-LBD group compared with controls (**Fig. 6f**), so are the viral loads shown by qRT-PCR and immunohistochemistry staining (**Fig. 6g and 6h**), confirming that soluble LRP8-LBD can block 17D infection and supporting its role as a receptor that directly binds YFV E on the virion surface.

Discussion

Virus receptors provide essential footholds for host-cell entry. Discovering them enables delineation of viral life cycles, interpretation of pathogenesis, and

291 development of therapies. LRP8 as a YFV host factor is conserved from
292 mosquitoes and ticks to non-human primates and humans. This suggests an
293 advantage to a one-receptor-for-many-hosts strategy, with fewer evolutionary
294 constraints. It is known that YFV 17D can infect the midgut of Aedes aegypti
295 mosquitoes but does not disseminate to the salivary glands and therefore
296 cannot be transmitted, suggesting a complex mechanism behind tissue tropism
297 and the possibility of other receptors involved in this vector[29,30]. Closest
298 relatives of YFV such as Sepik and Wesselsbron viruses do not appear to
299 engage LRP8. Recent work also suggests that tick-borne encephalitis virus
300 (TBEV) uses LRP8[31], and phylogenetic analysis indicates that LDLR-family
301 usage has arisen in distant virus families, likely via independent evolution
302 (**Extended Fig. 12**). Often multiple LDLR-family members can support entry for
303 a given virus. For YFV, our data indicate that, in addition to LRP8, LRP4 and
304 VLDLR can promote entry, possibly in different cells or tissues. This receptor
305 redundancy highlights the advantage of overexpression screens, which can
306 overcome redundancy that confounds loss-of-function approaches. That the
307 soluble LRP8 LBD can block YFV infection, together with prior studies, raises
308 the possibility of LRP8-based protein therapeutics or prophylactics for multiple
309 arboviruses. Finally, wild-type YFV strains such as Asibi or BJ01 do not respond
310 to mouse LRP8 or VLDLR as robustly as 17D, consistent with mice not being
311 the natural host and suggesting adaptation to mouse LRP8 during historical
312 passaging to generate 17D. These findings illuminate the evolutionary path
313 underlying one of the most successful vaccines and may inform prevention
314 strategies for other flaviviruses. Our data showing that expression of human
315 LRP8 in mouse livers can aggravate the pathogenesis may support an
316 improved mouse model of YFV infection with more consistent visceral
317 phenotype than the current mouse model[32].
318
319 **Acknowledgements**
320 This work was supported by a grant from the State Key Research Development
321 Program of China to X.T. (2021YFA1302503 and 2022YFE0102200). We thank
322 Lin Mei and Bin Luo for reagents, Wang L, Ding N and Yan X for technical
323 assistance, Zhang Yuhang and Zhang Guigen for editing the manuscript.
324
325 **Author contributions**
326 X.T. conceived and supervised the project. M. M., Y. Yang, Z. Zhang, Y. Yin, J.
327 T., J. C., Y. G., Z. W., D. W., Y. J., Y.C., H. W. conducted the experiments. Zhiyuan
328 Zhang, L. L. and Y. P. contributed computational analysis, R. L., Q. H., Z.D., Q.
329 H., C. S., Y. Z J. L., W. T., L. M. and G. C. provided reagents, guidance and
330 facility support. M.M. and X.T. wrote the manuscript with input from all other
331 authors.
332

Competing interests

The authors declare no competing interests.

Materials and Methods

Cells and viruses

We maintained HEK293T (human kidney epithelial, ATCC CRL-11268), HEK293FT (human kidney epithelial, Thermo Fisher Scientific, R70007), U87MG (human glioblastoma, ATCC HTB-14), Vero (Cercopithecus aethiops kidney, ATCC CCL-81), A549 (human lung epithelial, ATCC CCL-185), Huh7 (human hepatoma, CRL-10741), K562 (chronic myelogenous leukemia cell line, CCL-243), C6/36 (Aedes albopictus larva, ATCC CRL-1660), and BHK-21 (ATCC CCL-10) in DMEM (Gibco) supplemented with 10% fetal bovine serum (FBS), Primary human hepatocytes (Shenzhen Liver Biotechnology Co., Ltd.), 1% GlutaMAX (Thermo Fisher Scientific, 35050061), and 1% penicillin–streptomycin (Thermo Fisher Scientific, 151401148). We confirmed the absence of mycoplasma by monthly testing using myco-Lumi (Beyotime, C202985S) after ZellShield treatment (Minerva Biolabs, 13-0050).

Wild-type live flaviviruses used were YFV (clinical strain BJ01、Asibi and the live-attenuated vaccine strain YF17D) and ZIKV (strain SZ01). Viruses were propagated in C6/36 or Vero cells and titrated in BHK-21 by plaque assay.

Antibodies

Reagents included: anti-YFV Env (Creative Diagnostics, CABT-YN1194), anti-ZIKV Env (Creative Diagnostics, CABT-YN1207), LRP4 (Invitrogen, MA5-45577), LRP4 (GeneTex, GTX637988), ApoER2/LRP8 (Santa Cruz, sc-293472), Anti-VLDLR (GeneTex, GTX79552), LRP8 (Thermo Fisher, MA5-38566), ApoER2/LRP8 (Abclonal, A10517), pan-flavivirus Env (Creative Diagnostics, CABT-YN1131), 4G2 (Millipore, MAB10216), anti-Tim1 (Abclonal, A2831 and A26862), HRP-conjugated anti-rabbit (ZSGB-Bio, ZB-2301) anti-mouse (ZB-2305), and anti-human (W4038), Alexa Fluor 488 goat anti-mouse (A-11001), and Alexa Fluor 568 goat anti-rabbit (A-11011).

Reporter pseudovirus particle generation

To generate replication-incompetent reporter pseudovirus particles (RPPs), we used a DNA-based WNV replicon lacking the C-prM-E coding region (pWNVrep dCprME-GFP) co-transfected with a plasmid expressing flaviviral CprME. We cloned CprME of ZIKV strain SZ01 (GenBank KU866423), YF17D (GenBank OR509732), Asibi (GenBank MF405338), CNYF01 (GenBank KU921608), WESSV (GenBank NC_012735), SEPV (GenBank DQ837642), Dengue virus type 2 (GenBank NC_001474), WNV (GenBank NC_001563.2), JEV (GenBank NC_001437.1), and mutants into pcDNA3.1 under a CMV promoter. HEK293T

373 cells (5×10^6 per 15-cm dish) were seeded 12–18 h before transfection.
374 Standard medium (DMEM + 10% FBS, penicillin–streptomycin, GlutaMAX)
375 was used; cells were 50–60% confluent at transfection. We co-transfected 30
376 μg pWNVrep dCprME-GFP and 10 μg pcDNA3.1-CprME using Neofect
377 reagent, replaced medium at 8–12 h, and collected supernatants 3 days post-
378 transfection. Supernatants were centrifuged (4,000 rpm, 5 min), filtered (0.45
379 μm), and stored at −80 ° C.
380
381 For purification, supernatants at 48 and 72 h were clarified (4,000 rpm, 10 min)
382 and concentrated by Amicon Ultra-30 kDa units or purified on 10–60%
383 continuous sucrose gradients (200,000 g, 2 h). Bands were collected and
384 washed three times with ice-cold PBS using Amicon-30 kDa filters.
385 Preparations were stored at −80 °C (long-term) or 4 °C (≤2 weeks). Antigen
386 content was quantified by YFV ELISA (COIBIO, CB11927-Hu).

387 **Production and Purification of YF17D Live-Attenuated Virus**
388 YF17D was propagated in C6/36 at MOI 0.5 and 28 °C. Six days post-infection,
389 supernatant was harvested and centrifuged at 4,000 rpm for 30 min to remove
390 debris, filtered (0.45 μm), and precipitated with 40% PEG8000 at 4 °C overnight.
391 Pellets were collected (11,000 rpm, 30 min), resuspended in TNE buffer
392 (Shyuanye R20992), and purified by ultracentrifugation on a 24% sucrose
393 cushion (105,000 g, 2 h, 4 °C). Further purification used a 10–35% potassium
394 tartrate gradient (32,000 rpm, 2 h, 4 °C). Visible bands were collected and
395 concentrated by ultrafiltration (100 kDa MWCO).

396 **VLP labelling and imaging**
397 Purified YF17D or ZIKV VLPs were labelled with Alexa Fluor 647 NHS ester in
398 0.1 M sodium bicarbonate (pH 8.3) for 30 min at room temperature in the dark.
399 Reactions were quenched with 50 mM Tris–HCl (pH 7.5), and unbound dye
400 was removed by centrifugal filtration (100 kDa MWCO). Input was normalized
401 by envelope antigen content. HEK293T cells stably expressing luciferase, TIM1,
402 LRP8-ΔLBD, or LRP8 were used. Binding assays were performed at 4 °C for
403 45 min with six PBS/2% FBS washes; internalization was at 37 °C for 30 min
404 with optional proteinase K treatment (500 ng/mL, 15 min, 37 °C). Cells were
405 stained with FITC–WGA (5 μg/mL, 10 min, 4 °C) and DAPI, fixed in 4%
406 paraformaldehyde, and imaged by confocal microscopy. Single-cell VLP counts
407 were quantified using CellProfiler.
408

409 **Bio-layer interferometry analysis**
410 BLI analysis were performed at 25°C using an Octet R8 biosensor system
411 (Sartorius). YFV E antibody (GTX638626, GeneTex) was mixed and incubated
412 with biotin (#G-MM-IGT, Genemore) at a molar ratio of three biotins to one
413 protein at room temperature for 30min. Excess biotin was removed using a

414 desalting column(#G-MM-IGT, Genemore). Biotinylated protein (25μg·mL−1)
415 was immobilized onto the SA Biosensors (Sartorius #18-5019) for 3 min and
416 then used to capture YFV VLPs or YFV-17D viruses. The tips were washed
417 with the wash buffer (20 mM HEPES, 150 mM NaCl, pH 8.0) for 3 min to obtain
418 a baseline reading, then the biosensors were dipped into wells containing the
419 LRP8-Fc at various different concentrations for the indicated time. BLI data
420 analysis was performed by using the software Octet (version 12.2, Sartorius) in
421 the standard 1:1 binding mode. Raw binding data were exported and plotted in
422 GraphPad Prism8.0.
423

424 **Genome-wide ORF overexpression screen**

425 The pooled human ORF library contains 20,432 clonal ORFs mapping to
426 13,833 genes. HEK293T cells (1×10^7 per 150 mm dish) were transfected with
427 lentiviral ORF sublibraries and packaging plasmids (SV40 VSVg, Gag/Pol, TAT,
428 Rev; 1:1:1:1) using Neofect. Supernatants were collected at 36–48 h, aliquoted,
429 and stored at −80 °C. Sub-library titers were determined by puromycin selection.
430 Five million HEK293T cells were transduced at MOI 0.2, selected with
431 puromycin (2 μg/mL, 3 days), mixed in equal numbers, and infected with
432 YF17D-GFP at MOI 0.2 or mock-infected. At 24 hpi, GFP+ and GFP− cells were
433 sorted by FACS. Genomic DNA was extracted, barcodes amplified, and
434 sequenced (HiSeq-PE150). Reads were trimmed with Cutadapt, aligned with
435 Bowtie2, processed with SAMtools, counted with a custom Python script,
436 normalized with DESeq2, and log2 fold changes calculated relative to GFP−
437 samples. Scores integrated read counts and fold change (see Supplementary
438 Data Set).
439

440 **Viral entry assay**

441 For binding assays, HEK293T-Luc, HEK-LRP8iso3, U87MG-Cas9 only,
442 U87MG-sgNT, U87MG-sgLRP8-1, and U87MG-sgLRP8-2 cells (0.1 M per well,
443 24-well plates) were incubated with YF17D, BI01 and / or Asibi at MOI 1 at 4 °C
444 for 45 min and washed six times with ice-cold PBS/2% FBS. An anti-YFV Env
445 antibody (Creative Diagnostics, CABT-YN1194) served as a blocking control
446 (virus preincubated with 30× diluted antibody at 37 °C for 1 h). Cells were lysed
447 in RLT buffer (R4111, Magen) and RNA extracted for RT–qPCR. For
448 internalization, after binding and washing, prewarmed medium (37 °C, 2% FBS,
449 15 mM NH4Cl) was added and cells were incubated for 1 h at 37 °C. Residual
450 surface virions were removed with proteinase K (500 ng/mL, 15 min, 37 °C) and
451 ice-cold PBS/2% FBS before RNA extraction.
452

453 **Ectopic overexpression experiments**

454 For stable or transient expression assay, ORFs of LRP8 (GenBank
455 NM_017522.5), and LDL family: LRP3 (GenBank NM_002335.4), LRP4
456 (GenBank NM_002334.4), LRP5 (GenBank NM_002335.4), LRP6 (GenBank
457 NM_002336.3), LRP9 (GenBank NM_003105.6), LRP10 (GenBank
458 NM_014045.5), LRP11 (GenBank NM_032832.6), LRP12 (GenBank
459 NM_013437.5), LDLR (GenBank NM_000527.5), LDLRAD2 (GenBank
460 NM_001013693.3), LDLRAD3 (GenBank NM_174902.4), VLDLR (GenBank
461 NM_013703), CD209 (GenBank NM_021155.4), TIM1 (GenBank
462 NM_012206.3) were cloned into a CMV-driven lentivector with FLAG/HA tags.
463 Codon-optimized LRP1 (GenBank NM_002332), LRP2 (GenBank
464 NM_004525.3), *A. aegypti* LRP8 (GenBank XP_021711662), *Aedes albopictus*
465 VLDLR (GenBank XM_029869759.2), *Equus caballus* LRP8 (GenBank
466 XP_023485552), *Sturnus vulgaris* LRP8 (GenBank XM_014870608.1), *Canis*
467 *lupus familiaris* LRP8 (GenBank XM_038666202.1), *D. rodundus* bat LRP8
468 (GenBank XM_053920761.1), *Alligator mississippiensis* LRP8 (GenBank
469 XM_014598721.3), *Gallus chicken* LRP8 (GenBank NM_205186.3), *Ixodes*
470 *scapularis* VLDLR (GenBank XM_029983583.4), mouse LRP8 (GenBank
471 NM_001369051.1), mouse VLDLR (GenBank NM_013703.2), were
472 synthesized into pcDNA3.1 with C-terminal 3×HA. Lentiviral transduction and
473 puromycin selection (2 μg/mL, 3 days) generated stable lines. For HA-tagged
474 constructs, surface expression was confirmed by FACS using surface staining.
475 The target protein sequences from NCBI were downloaded and performed
476 multiple sequence alignment by Clustal W using the Geneious software
477 package.
478
479 **Genetic knockdown and knockout validation**
480 Specific siRNAs targeting LRP8 were synthesized by Jintuosi. In PHH cells
481 (Liver Biotechnology), 100nM siRNAs were transfected using RNAiMax. After
482 48 hours, the medium was replaced with PHH maintenance medium, and the
483 cells were infected with YF17D and BJ01. Another 48 hours later, the cells were
484 collected to detect viral RNA levels and the knockdown efficiency of LRP8
485 mRNA. The siRNA sequences are as follows:
486 siLRP8-1: CCUUGAAGAUGAUGGACUATT,
487 siLRP8-2: CTGGACTGACTCGGGCAATAA.
488 The single guide RNAs targeting LRP8 (Genebank NG011517) were designed
489 as follows,
490 F1, caccgCGTCACACTTCCACCGTTCG,
491 R1, aaacCGAACGGTGGAAGTGTGACGc;
492 F2: caccgACTGTCTGCACAGGTCTTCT,
493 R2: aaacAGAAGACCTGTGCAGACAGTc).
494 Then these guide RNAs were cloned into lenti-CRISPRv2 plasmid
495 (Addgen#52961). Lentivirus was collected from the supernatant of HEK293T

496 cells transfected with lenti-CRISPRv2 in addition of packaging plasmids
497 aforementioned. LRP8 knockout (KO) clones were generated by single guide
498 RNA in U87MG and selected with 2 μg/mL puromycin for 5-7 days. Further
499 sgLRP8 cells were pooled in 96-well plates at a density of 0.5 cell per well to
500 obtain single-cell clones. Each clone was validated by Western blot or Sanger
501 sequencing.
502

503 **Pull-down assay**

504 Purified soluble LRP8-Fc (10 μg) or isotype IgG was incubated with 30 μL
505 protein A/G magnetic beads (Thermo Fisher Scientific) in PBS/0.1% Tween-20
506 at 4 °C for 6 h. After removing unbound proteins, beads were incubated
507 overnight at 4 °C with clarified lysates from YF17D-infected Vero cells, washed
508 eight times with PBS/0.1% Tween-20, and eluted by boiling in SDS-PAGE
509 buffer for immunoblotting.

510

511 **Protein purification**
512 LRP8 LA1237 DNA was inserted into a vector encoding a C-terminal human
513 IgG Fc fusion and transfected into HEK293F (3.0×10^6 cells/mL). Supernatants
514 (60h after transfection) were purified on Protein A Sepharose 4B, washed with
515 20 mM HEPES/150 mM NaCl (pH 8.0), and eluted with 20 mM HEPES/150 mM
516 NaCl/0.1 M glycine (pH 2.8), followed by SEC (Superdex 200 10/300 GL) in 20
517 mM HEPES/150 mM NaCl (pH 8.0). LDLR-Fc was purified similarly. For VLDLR
518 LA1-8, co-transfection with RAP enabled on-column Ca2+-dependent refolding
519 after extensive EDTA washes.
520

521 **Decoy protein and antibody-mediated blocking assay**

522 Purified LRP8-Fc (200 μg/μL stock) or isotype IgG was serially diluted,
523 preincubated with YF17D or ZIKV (pseudovirus or live) at 37 °C for 1 h, then
524 added to cells. For pseudovirus, GFP+ cells were quantified at 24 h by
525 high-content imaging. For live virus, cells were fixed at 48 h and stained with
526 4G2 and fluorescent secondary antibodies. For antibody blocking, anti-LRP8 or
527 isotype controls were incubated with cells for 1 h at 37 °C before infection.
528

529 **Immunoblotting**
530 Cells and tissue samples were lysed in 1% NP-40 buffer on ice. Protein
531 concentrations were determined by BCA, samples denatured in 5× SDS-PAGE
532 buffer (10 min, 95 °C), resolved by SDS-PAGE, transferred to nitrocellulose,
533 blocked in TBST/5% milk, incubated with primary antibody overnight (4 °C),
534 washed, and probed with HRP-secondary antibodies for 1 h before detection.

535 **Immunofluorescence**

536 Eight thousand HEK293T or U87MG cells per well in 96-well plates were
537 infected with YF17D (MOI 0.3) or ZIKV SZ01 (MOI 0.2) for 24–48 h, fixed in 4%
538 paraformaldehyde, permeabilized with 0.2% Triton X-100 (Promega), and
539 stained with 4G2 (1:1000) and Alexa Fluor 488 secondary (Invitrogen, R37120,
540 1: 1000). Nuclei were counterstained with DAPI (Invitrogen, 62247, 1:10,000).
541 Images were acquired on a high-content microscope (Cytation 1) and infection
542 ratios quantified.
543

544 **Flow cytometry**

545 For membrane protein expression, cells were detached with 10 μM EDTA,
546 stained with anti-LRP8、anti-TIM1 or anti-HA for 30 min at room temperature,
547 washed, stained with AF-488 secondary for 1 h, fixed in 2% paraformaldehyde,
548 washed, and analyzed by flow cytometry. GFP+ cell ratios were quantified after
549 trypsinization for reporter assays.
550

551 **Quantitative real-time PCR**

552 DNA/RNA were extracted (Magen, R5111). Two micrograms of total RNA were
553 reverse-transcribed (ABM, G492). qPCR was performed with 2× ChamQ SYBR
554 reagents (Vazyme, Q321) on a Bio-Rad CFX96. qRT-PCR data were
555 normalized to GAPDH. The primer sets were as follows:
556 *GAPDH*-qF: CGGAGTCAACGGATTTGGTCGTAT;
557 *GAPDH*-qF: AGCCTTCTCCATGGTGGTGAAGAC;
558 *YF17D*-qF: ATGGCAGGAGGATTGTGGTG;
559 *YF17D*-qR: GTTGTGCGTCCTTGTGGAAC;
560 YFV BJ01-qF: GCTAATTGAGGTGYATTGGTCTGC;
561 YFV-BJ01-qR: CTGCTAATCGCTCAAMGAACG;
562 *YFV-Asibi*-qF*: GCACGGATGTAACAGACTGAAGA;*
563 *YFV-Asibi*-qR*: CCAGGCCGAACCTGTCAT;*
564 *LRP8*-qF: CCCATCCCTAATCTTCACCAAC;
565 *LRP8*-qR: CTAGTGCCACGACATTCTTGAG.
566

567 **In vivo mosquito experiments**

568 Four dsRNAs targeting the common region of Aedes aegypti VLDLR
569 (LOC5576021) and controls (luciferase, GFP) were designed (SnapDragon),
570 synthesized by in vitro transcription (MEGAscript, Ambion), and purified.
571 Female mosquitoes were chilled on ice and injected (1 μg/300 nl) into the thorax.
572 Gene silencing was verified by qRT-PCR. For infection, 1000 MID50 of YF17D
573 or ZIKV was microinjected. Mosquitoes were collected at 4 dpi for RT-qPCR.

Six pairs primers were synthysized as follows:
DS1 F: TAATACGACTCACTATAGGGATCCCCGTGATCATACCAAA
DS1 R: TAATACGACTCACTATAGGGCCAGTCCGTCCAGTACATCC
DS2 F: TAATACGACTCACTATAGGGAAACCTGCAGATCGGATGAG
DS2 R: TAATACGACTCACTATAGGGTTTTGCACTGGAACTGATCG
DS3 F: TAATACGACTCACTATAGGGCCTGCAGATCGGATGAGTTT
DS3 R: TAATACGACTCACTATAGGGGCAGGTTTTGTCCTTTTTGC
DS4 F:TAATACGACTCACTATAGGGGTATGCCGGGTTACCTGAGA
DS4 R: TAATACGACTCACTATAGGGTCAGAATCTTGCCCATGTTG
Ds-Luc-F: TAATACGACTCACTATAGGGGGACTTGGACACCGGTAAGA
Ds-Luc-R: TAATACGACTCACTATAGGGGTCCACGAACACAACACCAC
DS-GFP-F:TAATACGACTCACTATAGGGGTGAGCAAGGGCGAGGAG
DS-GFP-R:
TAATACGACTCACTATAGGGCATGATATAGACGTTGTGGCTGTT.

Mouse infection experiment

Five-week-old C57BL/6 mice were anesthetized and secured in a stereotaxic apparatus. For in vivo neutralization, YF17D was premixed with purified soluble LRP8-LBD-Fc or isotype IgG at 37℃ for 1 hours, each group contain six equal gender mice. Ten microliter (200 PFU) was injected into the lateral ventricle (AP +0.2 mm, ML ±1.0 mm, DV −2.0 mm) at 10–20 nL/s. The needle was left in place for 5–10 min to minimize backflow, and incisions were closed. Meloxicam (4 mg/kg, s.c.) was administered for three days. Survival was monitored daily. For viral quantification in brain infection and blood, another independant assay was performed, and all the mice were sacrificed at 10 days post infection, the blood and brain were collected.

In the AAV mouse model, 21 three-week-old AG129 mice were evenly divided into three groups, with equal numbers of males and females. Each mouse received a tail vein injection of 2×10^{11} gc of AAV2/8-TBG-LRP8, AAV2/8-TBG-LDLR, or an AAV2/8-TBG empty vector, packaged by CIBR Vector Core. Three weeks after AAV delivery, one mouse from each group was sacrificed to examine receptor expression in the liver. After confirming successful expression, each mouse was intraperitoneally injected with 10,000 PFU of BJ01, then weighed daily and monitored for health status. On the fifth day after YFV infection, blood was collected via the orbital vein to assess viremia, liver function markers, and inflammatory factors. When the mice were close to death, liver and brain tissues were collected to evaluate tissue viral titers and pathological changes. All animal procedures were Tsinghua or Shenzhen Third Hospital IACUC-approved and complied with institutional and national guidelines.

614 **Sera biochemistry analysis & ELISA analysis**

615 Alanine transaminase (ALT), Aspartate aminotransferase (AST) and Total
616 Bilirubin (TBIL) in mouse serum was detected using biochemistry assay kits
617 according to the corresponding instructions. All of the reagent kits were
618 manufactured by Nanjing Jian cheng Biotechnology Co., Ltd. The levels of and
619 MCP-1 in mouse serum were measured using commercial ELISA kits
620 manufactured by Sino Biological Biotechnology Co., Ltd. ALT detection kit
621 (C009-2-1, Nanjing Jiancheng Bioengineering Institute Co., Ltd)， AST
622 detection kit (C010-2-1, Nanjing Jiancheng Bioengineering Institute Co., Ltd)，
623 TBIL detection kit (C019-1-1, Nanjing Jiancheng Bioengineering Institute Co.,
624 Ltd)，MCP-1 ELISA kit (KIT50368, Sino Biological Biotechnology Co., Ltd).

625

626 **Immunohistochemistry**

627 After mouse sacrificed, the tissues were fixed in 4% paraformaldehyde
628 overnight at 4°C, then followed by 20%, 30% sucrose gradient dehydrated 1
629 day, embedded in OCT (SAKURA, 4583) and cut into 10 μm sections. For
630 Immunohistochemistry (IHC), antigen retrieval was performed by boiling in
631 0.01 M citrate buffer (pH 6.0) for 10 min. Endogenous hydrogen peroxidase
632 activity was blocked by 3% hydrogen peroxide in PBS for 30 min, followed by
633 incubating in primary antibodies overnight at 4 ℃, HRP-conjugated anti-rabbit
634 secondary antibody at RT (room temperature). DAB staining followed
635 instructions from the DAB detection kit (ZSGB-Bio, ZLI-9019) for 5–10 min at
636 RT, finally counter staining was performed using hematoxylin solution (Solarbio,
637 H8070). Primary antibodies and dilution factors are listed below: anti-YFV Env
638 (Creative Diagnostics, CABT-YN1194, 1:100), anti-LRP4 (GeneTex,
639 GTX637988, 1:100), anti-VLDLR (Abcam, ab302917, 1:100), LRP8 (Thermo
640 Fisher, MA5-38566, 1:100), anti-LRP8 (Abclonal, A10517, 1:50).

641

642 **Plaque assay for viral titer identification**

643 Supernatant titration (in PFU mL−1) of each HEK293T over-expressing cells
644 was obtained by plaque assay to determine the amount of infectious viral
645 particles (PFU). The virus titration was performed in BHK21 cells, and in DMEM
646 medium with 2% FBS. Briefly, 0.25× 10^6/mL BHK21 cells were seeded in each
647 well of a 12-well plate for 12h at 37°C to allow BHK21 cell adherence. Then, a
648 serial dilution of each virus stock from YFV subculture in DMEM medium
649 (without FBS, 1% penicillin/streptomycin, and 1% glutamine) was performed
650 from 10^{-1} to 10^{-7}. Then, 400 μL of each dilution was added in each well for virus
651 adsorption 1-2hr. After this, the virus was discarded and each well was overlaid
652 with 4mL 2% DMEM media containing final 0.8% complete LMP agarose. After

653 5 days of incubation at 37°C, the plaque visualization was made using 4% PFA
654 fixation and 0.2% crystal violet in 20% ethanol staining to visualize the plaques.

655

656 **Human liver and brain tissue collection**

657 Human liver tissue used in this study was collected from a patient who
658 underwent surgical resection for hepatic hemangioma. Human brain tissue
659 used in this study was collected from the unaffected area of a brain of a patient
660 who died of epilepsy. The collection protocol was approved by the Institutional
661 Review Board of Beijing Chao-Yang Hospital, Capital Medical University, and
662 written informed consent regarding tissue donation was obtained from the
663 patient and family before surgery.

664

665 **Human liver cell suspension preparation**

666 The tissue sample was minced into small pieces and incubated in digestion
667 buffer containing 1× PBS, collagenase D (1 mg ml−1, Sigma-Aldrich), dispase
668 (2.4 mg ml−1, Thermo Fisher Scien- tific), DNase (0.2 mg ml−1, Sigma-Aldrich)
669 and 3% heat-inactivated fetal bovine serum (FBS, Invitrogen) for 30 min at
670 37 °C. Cells suspensions were dissociated and passed through a 100 μm cell
671 strainer (BD).

672

673 **Cell preparation for scRNA-seq**

674 Thaw the cryovial containing frozen human liver single cells at 37℃, then
675 transfer suspension to a centrifuge tube with RPMI1640 (Gibco 11875119)+10%
676 FBS(Gibco 10100147C), centrifuged for 5 min at 300×g at 4°C. The cells were
677 resuspended in RPMI1640+2% FBS. Cell count and viability was estimated
678 using SeekMate Tinitan Fluorescence Cell Counter (SeekGene M002C) with
679 AO/PI reagent after removal erythrocytes (Solarbio R1010) and then debris and
680 dead cells removal was decided to be performed or not (Miltenyi 130-109-
681 398/130-090-101). Finally fresh cells were washed twice in the RPMI1640 and
682 then resuspended at 1×106 cells per ml in RPMI1640 and 2% FBS.

683

684 **Single cell RNA-seq library construction and sequencing**

685 Single-cell RNA-Seq libraries were prepared using SeekOne® DD Single Cell
686 3' library preparation kit (SeekGene Catalog No.K00202). Briefly, appropriate
687 number of cells were mixed with reverse transcription reagent and then added
688 to the sample well in SeekOne® chip S3. Subsequently, Barcoded Hydrogel

Beads (BHBs) and partitioning oil were dispensed into corresponding wells separately in chip S3. After emulsion droplet generation reverse transcription were performed at 42℃ for 90 minutes and inactivated at 85℃ for 5 minutes. Next, cDNA was purified from broken droplet and amplified in PCR reaction. The amplified cDNA product was then cleaned, fragmented, end repaired, A-tailed and ligated to sequencing adaptor. Finally, the indexed PCR were performed to amplified the DNA representing 3' polyA part of expressing genes which also contained Cell Barcode and Unique Molecular Index. The indexed sequencing libraries were cleanup with VAHTS DNA Clean Beads (Vazyme N411-01), analyzed by Qubit (Thermo Fisher Scientific Q33226) and Bio-Fragment Analyzer (Bioptic Qsep400). The libraries were then sequenced on GeneMind SURFSeq 5000 with PE150 read length.

Single cell RNA-seq data analysis

scRNA-seq data processing and analysis were conducted using Seurat (v5.3.0). Quality control was applied by retaining cells that met the following criteria: nFeature_RNA between 200 and 5000, nCount_RNA below 20000, and mitochondrial gene content less than 10%. This filtering step resulted in a total of 8271 cells. The data were subsequently normalized and scaled using the standard Seurat workflow. Expression values of the genes of interest were then extracted to generate visualizations and compute mean expression levels.

Data availability

ScRNA-seq raw data have been deposited in the Genome Sequence Archive (Genomics, Proteomics & Bioinformatics 2021) in National Genomics Data Center, China National Center for Bioinformation / Beijing Institute of Genomics, Chinese Academy of Sciences (GSA-Human: HRA013453).

Statistical analysis

Unless otherwise specified, experiments were repeated at least three times. Bar graphs show mean ± SEM. Unpaired two-tailed t-tests were used for p-values unless otherwise noted.

References

1 Bres, P. A century of progress in combating yellow fever. *Bulletin of the World Health Organization* **64**, 775-786 (1986).

2 Wax, R. G. Manipulation of Human History by Microbes. *Clinical Microbiology Newsletter* **29**, 9-16 (2007).

3 Staples, J. E. & Monath, T. P. Yellow fever: 100 years of discovery. *Jama-Journal of the American Medical Association* **300**, 960-962, doi:DOI 10.1001/jama.300.8.960 (2008).

4 Walter R, C. J., Agramonte A. The Etiology of Yellow Fever: An Additional Note. *Jama-Journal of the American Medical Association* **36**, 431-440 (1901).

5 Barrett, A. D. T. & Higgs, S. Yellow fever: A disease that has yet to be conquered. *Annu Rev Entomol* **52**, 209-229, doi:10.1146/annurev.ento.52.110405.091454 (2007).

6 *Yellow fever*, <https://www.who.int/news-room/fact-sheets/detail/yellow-fever> (2023).

7 Hansen, C. A. & Barrett, A. D. T. The Present and Future of Yellow Fever Vaccines. *Pharmaceuticals-Base* **14**, doi:ARTN 89110.3390/ph14090891 (2021).

8 Meier, K. C., Gardner, C. L., Khoretonenko, M. V., Klimstra, W. B. & Ryman, K. D. A Mouse Model for Studying Viscerotropic Disease Caused by Yellow Fever Virus Infection. *Plos Pathog* **5**, doi:ARTN e100061410.1371/journal.ppat.1000614 (2009).

9 Vasconcelos, P. F. C. & Monath, T. P. Yellow Fever Remains a Potential Threat to Public Health. *Vector-Borne Zoonot* **16**, 566-567, doi:10.1089/vbz.2016.2031 (2016).

10 Orenstein, W. A., Offit, P. A., Edwards, K. M. & Plotkin, S. A. *Plotkin's vaccines*. 8th edition. edn, (Elsevier, 2024).

11 Wang, H. J. *et al.* Development of a Bicistronic Yellow Fever Live Attenuated Vaccine with Reduced Neurovirulence and Viscerotropism. *Microbiol Spectr* **10**, doi:10.1128/spectrum.02246-22 (2022).

12 Davis, E. H. *et al.* Impact of yellow fever virus envelope protein on wild-type and vaccine epitopes and tissue tropism. *Npj Vaccines* **7**, doi:ARTN 3910.1038/s41541-022-00460-6 (2022).

13 Lee, E. & Lobigs, M. E protein domain III determinants of yellow fever virus 17D vaccine strain enhance binding to glycosaminoglycans, impede virus spread, and attenuate virulence. *J Virol* **82**, 6024-6033, doi:10.1128/Jvi.02509-07 (2008).

14 Zhang, J. Y. *et al.* Amino acid changes in two viral proteins drive attenuation of the yellow fever 17D vaccine. *Nat Microbiol* **10**, doi:10.1038/s41564-025-02047-y (2025).

15 Nickells, J. *et al.* Neuroadapted Yellow Fever Virus Strain 17D: a Charged Locus in Domain III of the E Protein Governs Heparin Binding Activity and

768 Neuroinvasiveness in the SCID Mouse Model. *J Virol* **82**, 12510-12519,
769 doi:10.1128/Jvi.00458-08 (2008).
770 16 Fernandez-Garcia, M. D. *et al.* Vaccine and Wild-Type Strains of Yellow
771 Fever Virus Engage Distinct Entry Mechanisms and Differentially Stimulate
772 Antiviral Immune Responses. *Mbio* **7**, doi:ARTN e01956-
773 1510.1128/mBio.01956-15 (2016).
774 17 Douam, F. & Ploss, A. Yellow Fever Virus: Knowledge Gaps Impeding the
775 Fight Against an Old Foe. *Trends Microbiol* **26**, 913-928,
776 doi:10.1016/j.tim.2018.05.012 (2018).
777 18 Sack, L. M. *et al.* Profound Tissue Specificity in Proliferation Control Underlies
778 Cancer Drivers and Aneuploidy Patterns. *Cell* **173**, 499-+, doi:ARTN
779 514.e110.1016/j.cell.2018.02.037 (2018).
780 19 Li, S. *et al.* Gain-of-function genetic screening identifies the antiviral function
781 of TMEM120A via STING activation. *Nat Commun* **13**, 105,
782 doi:10.1038/s41467-021-27670-1 (2022).
783 20 Pierson, T. C. *et al.* A rapid and quantitative assay for measuring antibody-
784 mediated neutralization of West Nile virus infection. *Virology* **346**, 53-65,
785 doi:10.1016/j.virol.2005.10.030 (2006).
786 21 Herz, J. The LDL receptor gene family: (Un)expected signal transducers in
787 the brain. *Neuron* **29**, 571-581, doi:Doi 10.1016/S0896-6273(01)00234-3
788 (2001).
789 22 Kim, D. H. *et al.* Human apolipoprotein E receptor 2 - A novel lipoprotein
790 receptor of the low density lipoprotein receptor family predominantly
791 expressed in brain. *J Biol Chem* **271**, 8373-8380, doi:DOI
792 10.1074/jbc.271.14.8373 (1996).
793 23 Novak, S., Hiesberger, T., Schneider, W. J. & Nimpf, J. A new low density
794 lipoprotein receptor homologue with 8 ligand binding repeats in brain of
795 chicken and mouse (vol 271, pg 11732, 1996). *J Biol Chem* **271**, 27188-
796 27188 (1996).
797 24 Clark, L. E. *et al.* VLDLR and ApoER2 are receptors for multiple alphaviruses.
798 *Nature* **602**, 475-+, doi:10.1038/s41586-021-04326-0 (2022).
799 25 Meertens, L. *et al.* The TIM and TAM Families of Phosphatidylserine
800 Receptors Mediate Dengue Virus Entry. *Cell Host Microbe* **12**, 544-557,
801 doi:10.1016/j.chom.2012.08.009 (2012).
802 26 Hirai, H. *et al.* Structural basis for ligand capture and release by the endocytic
803 receptor ApoER2. *Embo Rep* **18**, 982-999, doi:10.15252/embr.201643521
804 (2017).
805 27 Li, M. *et al.* Rift Valley Fever Virus and Yellow Fever Virus in Urine: A
806 Potential Source of Infection. *Virol Sin* **34**, 342-345, doi:10.1007/s12250-019-
807 00096-2 (2019).
808 28 Pierson, T. C., Lazear H.M., Diamond M.S. in *Fields Virology* Vol. 1 (ed P.M.
809 Howley, Knipe, D.M.) Ch. 9, volumes (Wolters Kluwer, 2021).

29 Danet, L. *et al.* Midgut barriers prevent the replication and dissemination of the yellow fever vaccine in. *Plos Neglect Trop D* **13**, doi:ARTN e000729910.1371/journal.pntd.0007299 (2019).
30 Bellone, R., Mousson, L., Bohers, C., Mantel, N. & Failloux, A. B. Absence of transmission of vYF next generation Yellow Fever vaccine in mosquitoes. *Plos Neglect Trop D* **16**, doi:ARTN e001093010.1371/journal.pntd.0010930 (2022).
31 Mittler, E. *et al.* LRP8 is a receptor for tick-borne encephalitis virus. *Nature* **646**, doi:10.1038/s41586-025-09500-2 (2025).
32 Erickson, A. K. & Pfeiffer, J. K. Spectrum of disease outcomes in mice infected with YFV-17D. *Journal of General Virology* **96**, 1328-1339, doi:10.1099/vir.0.000075 (2015).

Figure legends

Figure 1. Human genome-wide ORFeome library screening identifies LRP8 as a YFV receptor. **a,** Schematic of the workflow of the screen. **b,** Deep-sequencing analysis of the screen performed with YF17D-GFP in HEK293T cells stably expressing the human ORFeome library. The x-axis shows log2 fold change of a gene's read counts in GFP+ versus GFP− cells; the y-axis shows −log10 p-values. **c-e,** Luciferase, LDLR, LRP8, or TIM1 were expressed in HEK293T cells and infected with YF17D, ZIKV, Dengue virus 2, WNV, JEV, SEPV or WESSV pseudoviruses. Blue and green indicate DAPI and GFP, respectively. **d**, Quantification of **c**. **e**, Supernatants from HEK293T overexpressing luciferase or LRP8 infected by live YF17D virus at 48 hpi were collected and the viral titers were determined using palque assay in BHK21 cells. **f-g**, Ectopic LRP8 expression enhanced infection of YF17D (MOI 0.1) (**e**) and BJ01 (MOI 0.01) (**f**) shown in a time course. Viral RNA was normalized to GAPDH. h. HEK293T cells were transfected with the indicated genes were infected with the indicated pseudoviruses for 48h before being analyzed by FACS. Statistical analysis was performed using one-way analysis of variance (ANOVA) with Dunnett's multiple comparisons test(d), two-tailed unpaired t-tests (e, f, g).The statistics shown are Mean ± SEM. *: $P < 0.05$; **: $P < 0.01$; ***: $P < 0.001$; ****: $P < 0.0001$, ns, not significant. The replicate in the figure indicates biological replicates, the experiments were repeated at least three times.

Figure 2. YFV infection requires LRP8 in U87-MG cells. **a**, Cas9/sgRNAs or Cas9 only were expressed in U87MG; single clones were selected. Knockout cells were infected with 17D-GFP for two days and analyzed by Western blot. sgNT: non-targeting sgRNA; sgLRP8-1/2: sgRNAs targeting human LRP8. **b–**

852 **c**, LRP8 knockout cells or control cells were infected with live 17D or ZIKV for
853 two days, fixed, stained with 4G2 and DAPI, imaged, and quantified. **d-e**,
854 Knockout cells were infected with the clinical BJ01 (0.2moi), viral RNA was
855 quantified by RT–qPCR and viral titer was quantified by focus-forming assay.
856 **f–h**, U87MG LRP8-KO cells were reconstituted with LRP8 WT or LRP8-ΔLBD
857 by electroporation and infected with 17D-GFP or ZIKV-GFP; imaging and
858 quantification as above. **h**, Western blot analysis of LRP8 and GFP as in the
859 17D-GFP infected group of **f**. **i**, U87MG cells pretreated with an anti-LRP8
860 antibody or isotype IgG were infected with YF17D or ZIKV and quantified by
861 4G2 staining. Statistical analysis was performed using one-way analysis of
862 variance (ANOVA) with Dunnett's multiple comparisons test(d,e), two-way
863 analysis of variance (ANOVA) with Turkey's multiple comparisons test (c, g).
864 The statistics shown are Mean ± SEM. *: P < 0.05; **: P < 0.01; ***: P < 0.001;
865 ****: P < 0.0001，ns, not significant. The replicate in the figure indicates
866 biological replicates, the experiments were repeated at least three times.
867
868 **Figure 3**. LRP8 promotes YFV entry by binding to its envelope protein. **a**,
869 HEK293T cells stably expressing luciferase or LRP8 were infected with YF17D
870 at MOI 1 either at 4 °C for 45 min to measure binding or at 37 °C for 1 h to
871 measure internalization. **b–c**, U87MG LRP8-KO and Cas9-only control cells
872 were tested similarly; a pan-flavivirus E antibody served as a blocking control.
873 **d–f**, HEK293T cells expressing LRP8, LRP8-ΔLBD, TIM1, or luciferase were
874 treated with Alexa Fluor 647–labeled VLPs bearing YFV 17D E (**d, e**) or ZIKV
875 E (**f**). FITC–WGA was added to label cell membranes before imaging. **g**,
876 Pulldown of YF17D E protein by immobilized LRP8 LBD-Fc. **h, i,** BLI
877 measurement of immobilized live YF17D (**h**) or YF17D VLP (**i**) binding to
878 soluble LRP8-LBD. Statistical analysis was performed using two-tailed
879 unpaired t-tests (a), one-way analysis of variance (ANOVA) with Dunnett's
880 multiple comparisons test(b, c), two-way analysis of variance (ANOVA) with
881 Turkey's multiple comparisons test (d, f). The statistics shown are Mean ± SEM.
882 *: P < 0.05; **: P < 0.01; ***: P < 0.001; ****: P < 0.0001，ns, not significant.
883 The replicate in the figure indicates biological replicates, the experiments were
884 repeated at least three times.
885
886 **Figure 4**. Effects of LDLR family members and LRP8 homologs on YFV
887 infection. **a, b, c**, HEK293T cells transfected with LDLR family members were
888 infected with YF17D-GFP or BJ01 or Asibi for 48 h and analyzed by
889 fluorescence microscopy (YF17D-GFP) or qRT-PCR (BJ01 and Asibi). **d**, **e**,
890 LRP8 homologs from different species were expressed in HEK293T cells and
891 infected with YF17D-GFP or BJ01 for 48 h and analyzed by fluorescence
892 microscopy (YF17D-GFP) or qRT-PCR (BJ01). Statistical analysis was
893 performed using one-way analysis of variance (ANOVA) with Dunnett's multiple

894 comparisons test (a-e). The statistics shown are Mean ± SEM. *: P < 0.05; **:
895 P < 0.01; ***: P < 0.001; ****: P < 0.0001，ns, not significant. The replicate in
896 the figure indicates biological replicates, the experiments were repeated at least
897 three times.
898
899 **Figure 5**. LRP8 is expressed in human liver and mediates YFV infection in
900 primary human hepatocytes and in a mouse model. **a**, LRP8, LRP4 and VLDLR
901 expression were determined in human brain or liver by immunohistochemistry
902 staining with corresponding antibodies. **b**, Scaled expression levels of LRP8,
903 LRP4 and VLDLR in human liver single cell RNAseq data. The red dot within
904 each column represents the mean expression value across all cells. **c**, Western
905 blots of human liver samples, including crude liver lysates, showed clear LRP8
906 expression at levels comparable to brain. HEK293T cells overexpressing one
907 of the three genes were included as controls showing the specificity of the
908 antibodies. **d-i**, Primary human hepatocytes were transfected with siRNAs
909 targeting LRP8 or non-targeting control siRNAs (NC-1 and NC-2) for 48 hours
910 and infected with live YF17D (**d-f**) or BJ01 (**g, i**) for 48 hour, and the viral RNA
911 and LRP8 mRNA level from cell total RNA were quantified via qRT-PCR (**d, f,**
912 **g, j**). The virus titers of the supernatant were quantified by plaque assay (**e, h**).
913 **j-p**, In AG129 mice, 2x 10^{11} genome-copies of AAV-TBG expressing either
914 LRP8 or LDLR and an empty AAV were injected by tail vein into each mouse.
915 Three weeks later, YFV BJ01 was injected intraperitoneally. The survival curve
916 of the mice were shown in j. Five days post YFV injection, the blood was drawn
917 from the mice to measure viral load (**k**) and levels of ALT and AST enzymatic
918 activities and levels of bilirubin and MCP-1 (**i-o**). The livers of a mock mouse
919 and two mice each from the LDLR and LRP8 group died at day 7 (LRP8 group)
920 or day 10 (LDLR group) were processed for immunohistochemistry imaging
921 with DAB staining of YFV E protein with an anti-E antibody, asterisks indicate
922 sites of positive staining (**p**). Statistical analysis was performed using one-way
923 analysis of variance (ANOVA) with Dunnett's multiple comparisons test (b, d-i,
924 k-o),log-rank (Mantal Cox) test (j). The statistics shown are Mean ± SEM. *: P
925 < 0.05; **: P < 0.01; ***: P < 0.001; ****: P < 0.0001，ns, not significant. The
926 replicate in the figure indicates biological replicates, the experiments were
927 repeated at least twice.
928
929 **Figure 6**. LRP8 function in YFV infection in animal models. **a–b**, *Aedes aegypti*
930 mosquitoes injected with dsRNA targeting VLDLR or control dsRNA for three
931 days were then infected with YF17D. Four days post infection, viral RNA (**a**)
932 and VLDLR mRNA (**b**) were quantified by qRT–qPCR. **c–d**, dsRNA-treated
933 mosquitoes were infected with ZIKV. **e**, YF17D or 17D-GFP was treated with
934 soluble LRP8 LBD-Fc or isotype IgG and used to infect U87MG cells; infection
935 was quantified by immunofluorescence or GFP. **f**, C57BL/6 mice were injected

936 intracerebrally with YF17D preincubated with LRP8 LBD-Fc or isotype IgG;
937 survival was recorded daily. **g**. Brain from mice of **f** was drawn to measure viral
938 load by qRT-PCR. **h**. In a repeat experiment of **f**. mice at day 10 post infection
939 were sacrificed and the brain of the mice were processed for
940 immunohistochemistry imaging with DAB staining of YFV E protein with an anti-
941 E antibody. Statistical analysis was performed using one-way analysis of
942 variance (ANOVA) with Dunnett's multiple comparisons test (a-d), log-rank
943 (Mantal Cox) test (f), two-tailed unpaired t-test with Welch's correction (g). The
944 statistics shown are Mean ± SEM. *: $P < 0.05$; **: $P < 0.01$; ***: $P < 0.001$; ****:
945 $P < 0.0001$，ns, not significant. The replicate in the figure indicates biological
946 replicates, the experiments were repeated at least twice.
947
948

Fig.1

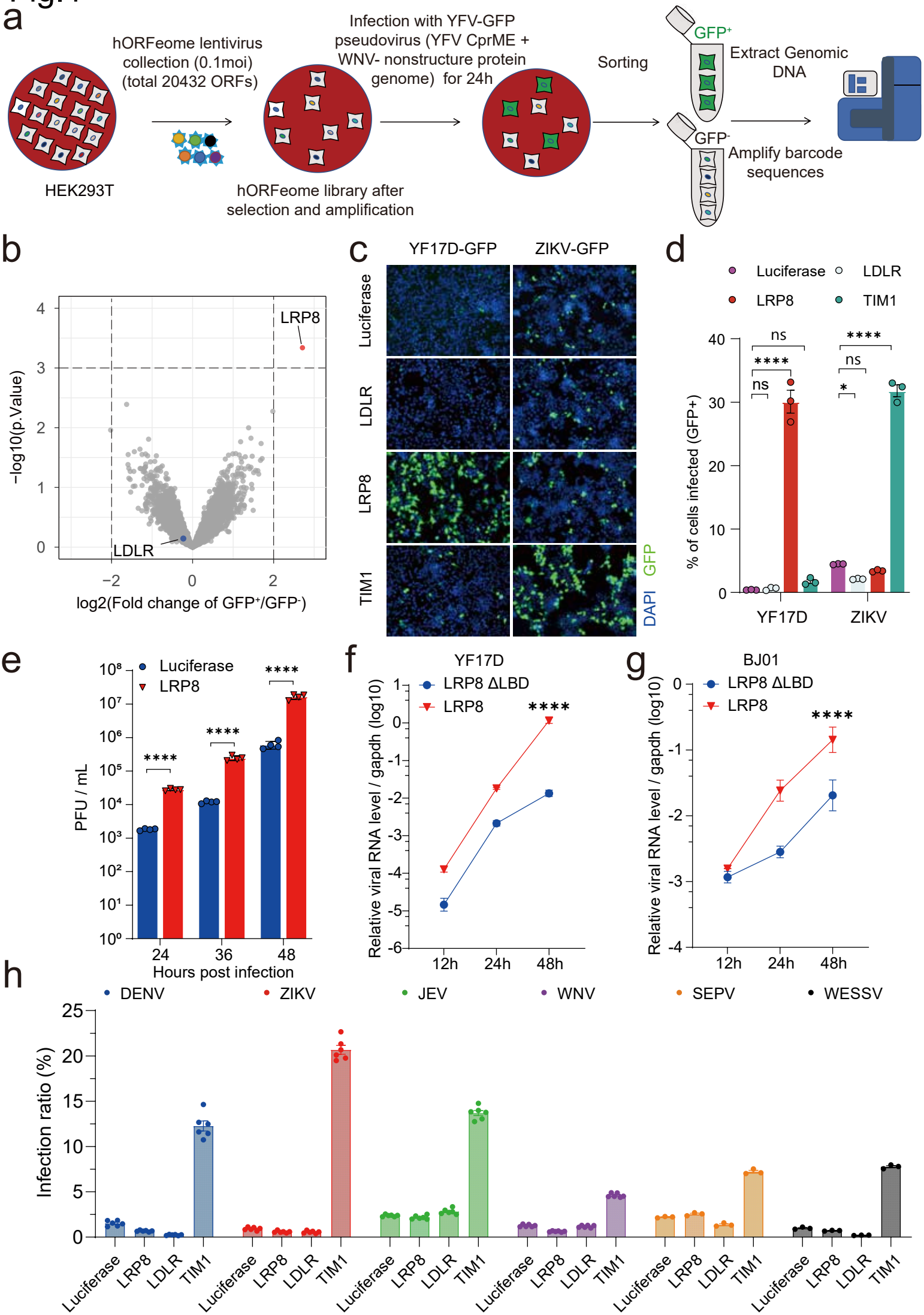
a
hORFeome lentivirus collection (0.1moi) (total 20432 ORFs)
Infection with YFV-GFP pseudovirus (YFV CprME + WNV- nonstructure protein genome) for 24h
Sorting
GFP+
GFP-
Extract Genomic DNA
Amplify barcode sequences
HEK293T
hORFeome library after selection and amplification
b
LRP8
LDLR
−log10(p.Value)
log2(Fold change of GFP+/GFP-)
c
YF17D-GFP
ZIKV-GFP
Luciferase
LDLR
LRP8
TIM1
GFP
DAPI
d
Luciferase
LDLR
LRP8
TIM1
% of cells infected (GFP+)
ns
****
*
YF17D
ZIKV
e
Luciferase
LRP8
PFU / mL
Hours post infection
f
YF17D
LRP8 ΔLBD
LRP8
Relative viral RNA level / gapdh (log10)
12h
24h
48h
g
BJ01
LRP8 ΔLBD
LRP8
h
DENV
ZIKV
JEV
WNV
SEPV
WESSV
Infection ratio (%)
Luciferase
LRP8
LDLR
TIM1

Fig.2

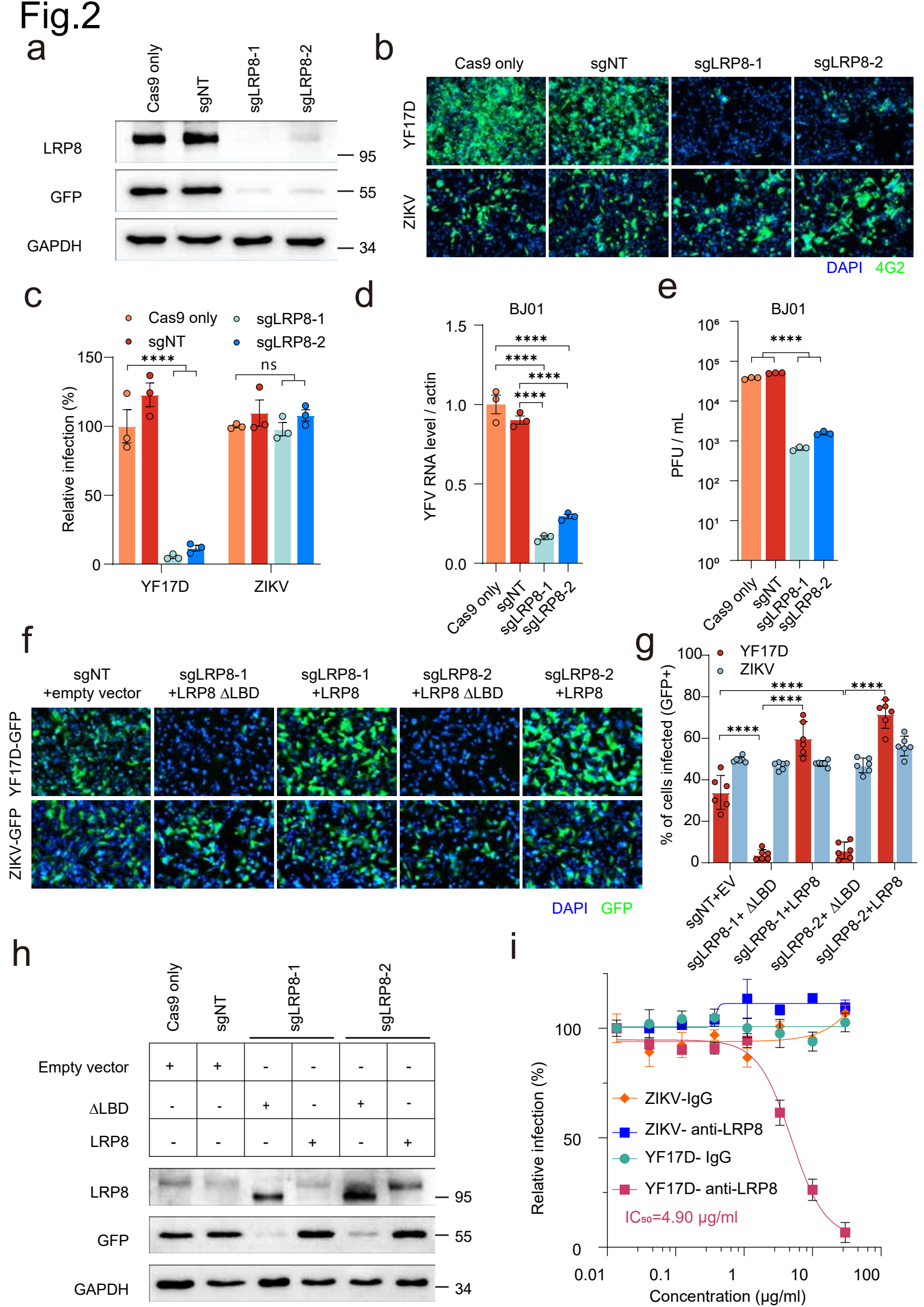
a
Cas9 only
sgNT
sgLRP8-1
sgLRP8-2
LRP8
GFP
GAPDH
95
55
34
b
Cas9 only
sgNT
sgLRP8-1
sgLRP8-2
YF17D
ZIKV
DAPI 4G2
c
Cas9 only
sgNT
sgLRP8-1
sgLRP8-2
Relative infection (%)
150
100
50
0
****
ns
YF17D
ZIKV
d
BJ01
YFV RNA level / actin
1.5
1.0
0.5
0.0
****
Cas9 only
sgNT
sgLRP8-1
sgLRP8-2
e
BJ01
PFU / mL
10^6
10^5
10^4
10^3
10^2
10^1
10^0
****
Cas9 only
sgNT
sgLRP8-1
sgLRP8-2
f
sgNT +empty vector
sgLRP8-1 +LRP8 ΔLBD
sgLRP8-1 +LRP8
sgLRP8-2 +LRP8 ΔLBD
sgLRP8-2 +LRP8
YF17D-GFP
ZIKV-GFP
DAPI GFP
g
YF17D
ZIKV
% of cells infected (GFP+)
100
80
60
40
20
0
****
sgNT+EV
sgLRP8-1+ ΔLBD
sgLRP8-1+LRP8
sgLRP8-2+ ΔLBD
sgLRP8-2+LRP8
h
Cas9 only
sgNT
sgLRP8-1
sgLRP8-2
Empty vector
ΔLBD
LRP8
LRP8
GFP
GAPDH
95
55
34
i
Relative infection (%)
100
50
0
ZIKV-IgG
ZIKV- anti-LRP8
YF17D- IgG
YF17D- anti-LRP8
IC50=4.90 μg/ml
0.01
0.1
1
10
100
Concentration (μg/ml)

Fig.3

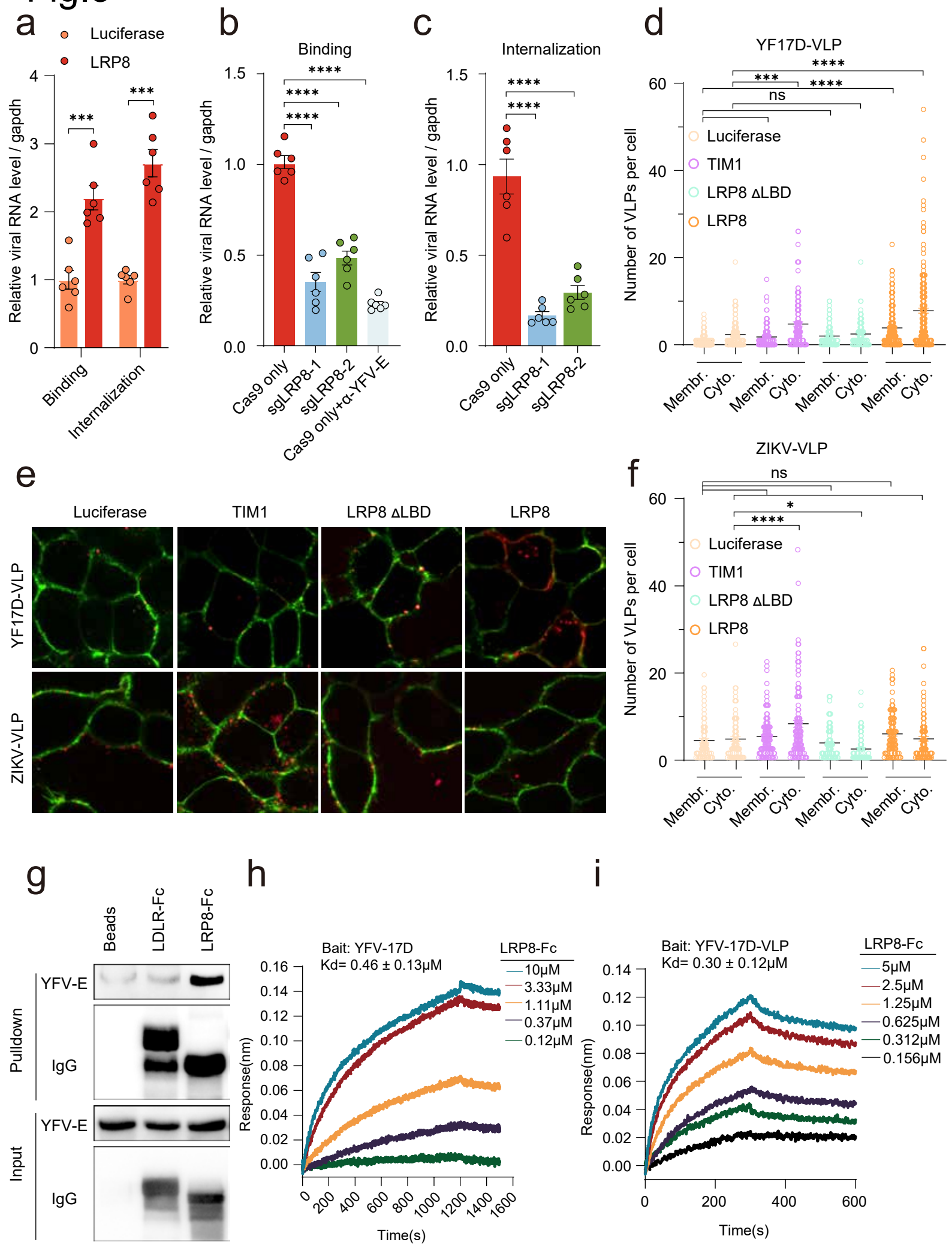
a
Luciferase
LRP8
Relative viral RNA level / gapdh
***
***
Binding
Internalization
b
Binding
Relative viral RNA level / gapdh
****
****
****
Cas9 only
sgLRP8-1
sgLRP8-2
Cas9 only+α-YFV-E
c
Internalization
Relative viral RNA level / gapdh
****
****
Cas9 only
sgLRP8-1
sgLRP8-2
d
YF17D-VLP
Number of VLPs per cell
****
***
****
ns
Luciferase
TIM1
LRP8 ΔLBD
LRP8
Membr.
Cyto.
e
Luciferase
TIM1
LRP8 ΔLBD
LRP8
YF17D-VLP
ZIKV-VLP
f
ZIKV-VLP
Number of VLPs per cell
ns
*
****
Luciferase
TIM1
LRP8 ΔLBD
LRP8
Membr.
Cyto.
g
Beads
LDLR-Fc
LRP8-Fc
Pulldown
YFV-E
IgG
Input
YFV-E
IgG
h
Bait: YFV-17D
Kd= 0.46 ± 0.13μM
LRP8-Fc
10μM
3.33μM
1.11μM
0.37μM
0.12μM
Response(nm)
Time(s)
i
Bait: YFV-17D-VLP
Kd= 0.30 ± 0.12μM
LRP8-Fc
5μM
2.5μM
1.25μM
0.625μM
0.312μM
0.156μM
Response(nm)
Time(s)

Fig.4

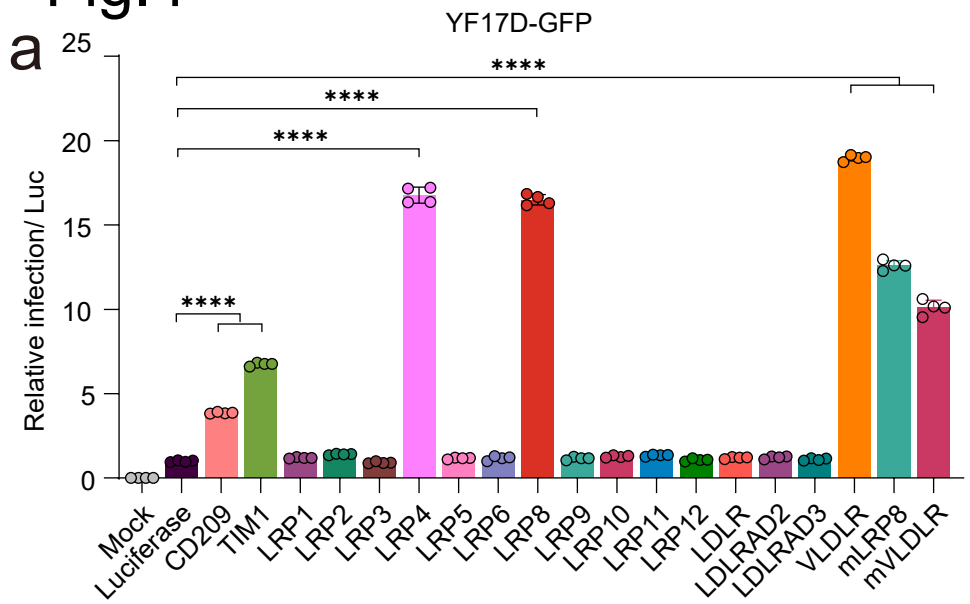
a
YF17D-GFP
Relative infection/ Luc
0
5
10
15
20
25
****
****
****
****
Mock
Luciferase
CD209
TIM1
LRP1
LRP2
LRP3
LRP4
LRP5
LRP6
LRP8
LRP9
LRP10
LRP11
LRP12
LDLR
LDLRAD2
LDLRAD3
VLDLR
mLRP8
mVLDLR

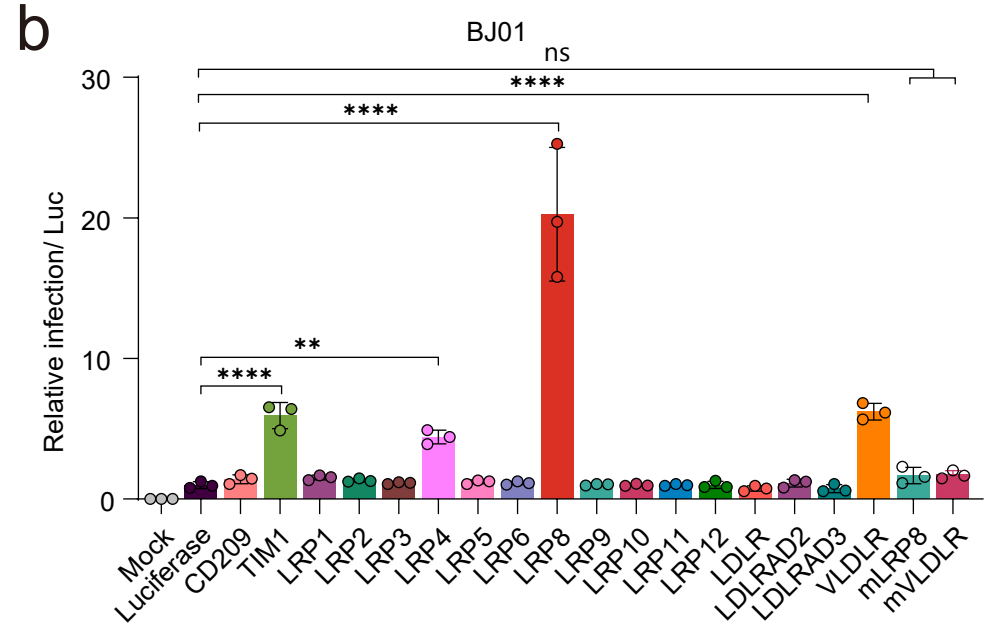
b
BJ01
Relative infection/ Luc
0
10
20
30
ns
****
****
**
****
Mock
Luciferase
CD209
TIM1
LRP1
LRP2
LRP3
LRP4
LRP5
LRP6
LRP8
LRP9
LRP10
LRP11
LRP12
LDLR
LDLRAD2
LDLRAD3
VLDLR
mLRP8
mVLDLR

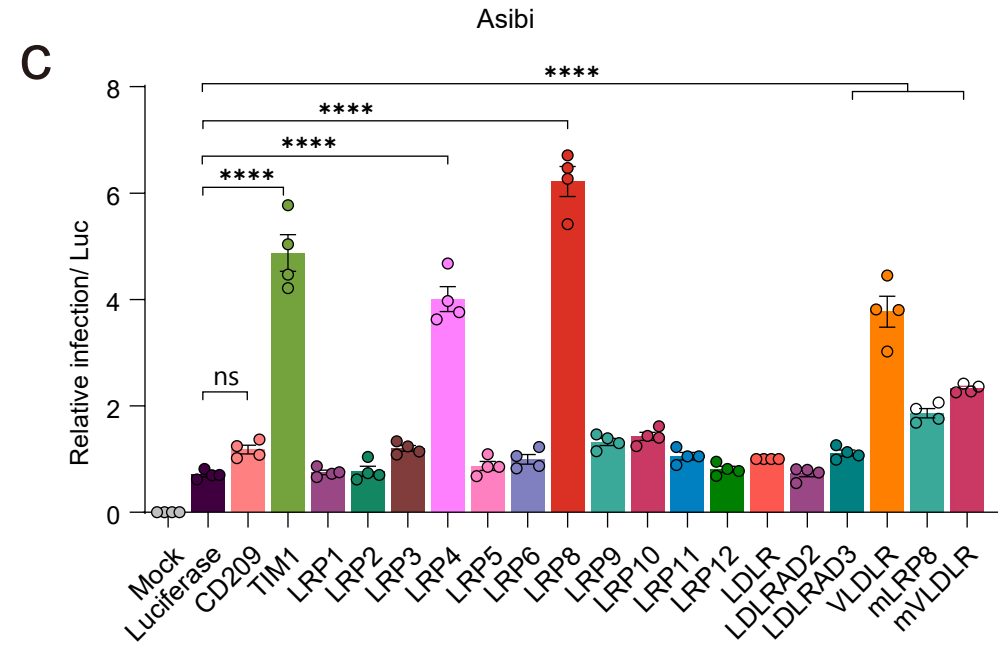
c
Asibi
Relative infection/ Luc
0
2
4
6
8
****
****
****
****
ns
Mock
Luciferase
CD209
TIM1
LRP1
LRP2
LRP3
LRP4
LRP5
LRP6
LRP8
LRP9
LRP10
LRP11
LRP12
LDLR
LDLRAD2
LDLRAD3
VLDLR
mLRP8
mVLDLR

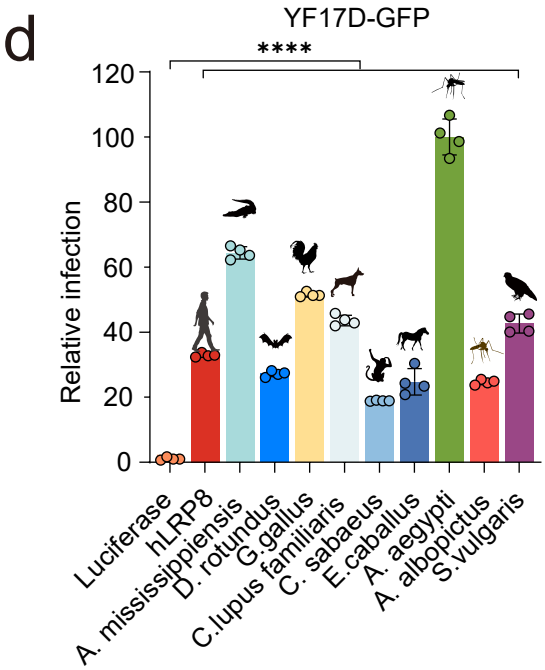
d
YF17D-GFP
Relative infection
0
20
40
60
80
100
120
****
Luciferase
hLRP8
A. mississippiensis
D. rotundus
G.gallus
C.lupus familiaris
C. sabaeus
E.caballus
A. aegypti
A. albopictus
S.vulgaris

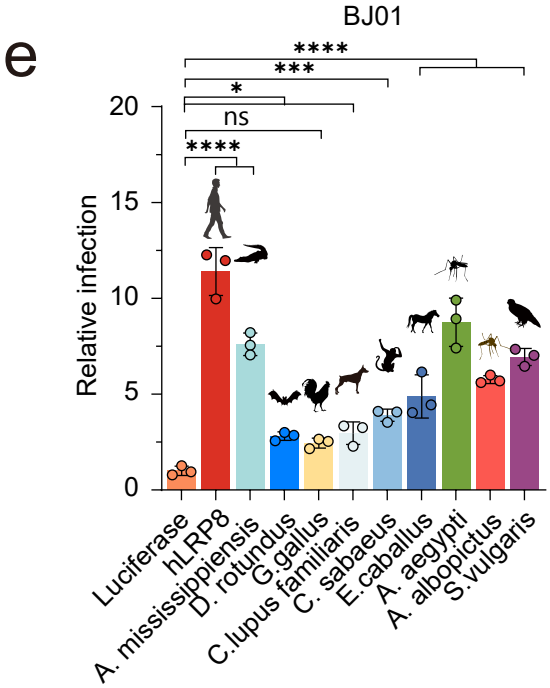
e
BJ01
Relative infection
0
5
10
15
20
****
***
*
ns
****
Luciferase
hLRP8
A. mississippiensis
D. rotundus
G.gallus
C.lupus familiaris
C. sabaeus
E.caballus
A. aegypti
A. albopictus
S.vulgaris

Fig.5

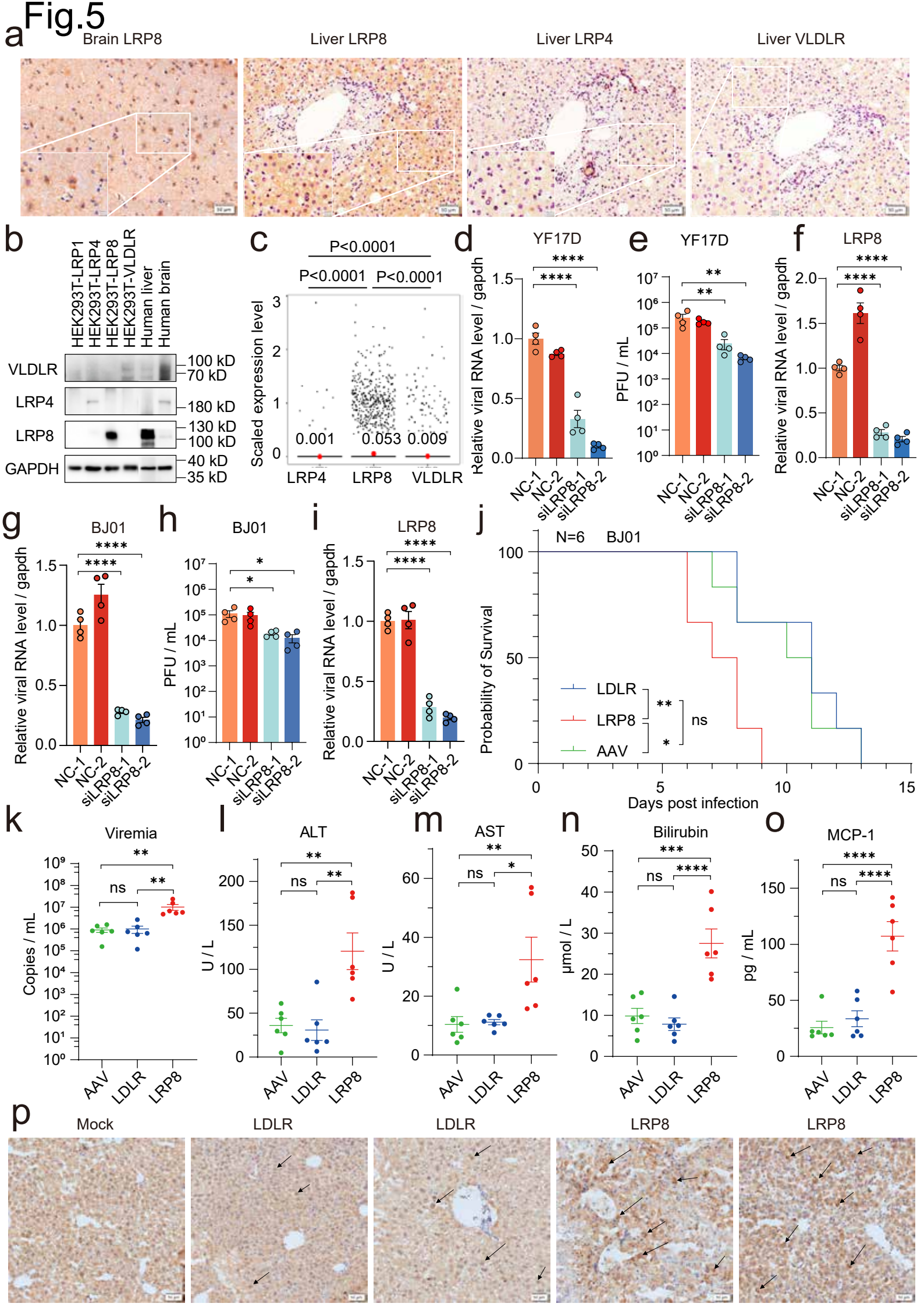
a
Brain LRP8
Liver LRP8
Liver LRP4
Liver VLDLR
b
HEK293T-LRP1
HEK293T-LRP4
HEK293T-LRP8
HEK293T-VLDLR
Human liver
Human brain
VLDLR
LRP4
LRP8
GAPDH
100 kD
70 kD
180 kD
130 kD
100 kD
40 kD
35 kD
c
P<0.0001
P<0.0001
P<0.0001
Scaled expression level
0.001
0.053
0.009
LRP4
LRP8
VLDLR
d
YF17D
Relative viral RNA level / gapdh
NC-1
NC-2
siLRP8-1
siLRP8-2
e
YF17D
PFU / mL
f
LRP8
Relative viral RNA level / gapdh
g
BJ01
Relative viral RNA level / gapdh
h
BJ01
PFU / mL
i
LRP8
Relative viral RNA level / gapdh
j
N=6 BJ01
Probability of Survival
Days post infection
LDLR
LRP8
AAV
ns
k
Viremia
Copies / mL
AAV
LDLR
LRP8
l
ALT
U / L
m
AST
U / L
n
Bilirubin
μmol / L
o
MCP-1
pg / mL
p
Mock
LDLR
LDLR
LRP8
LRP8

Fig.6

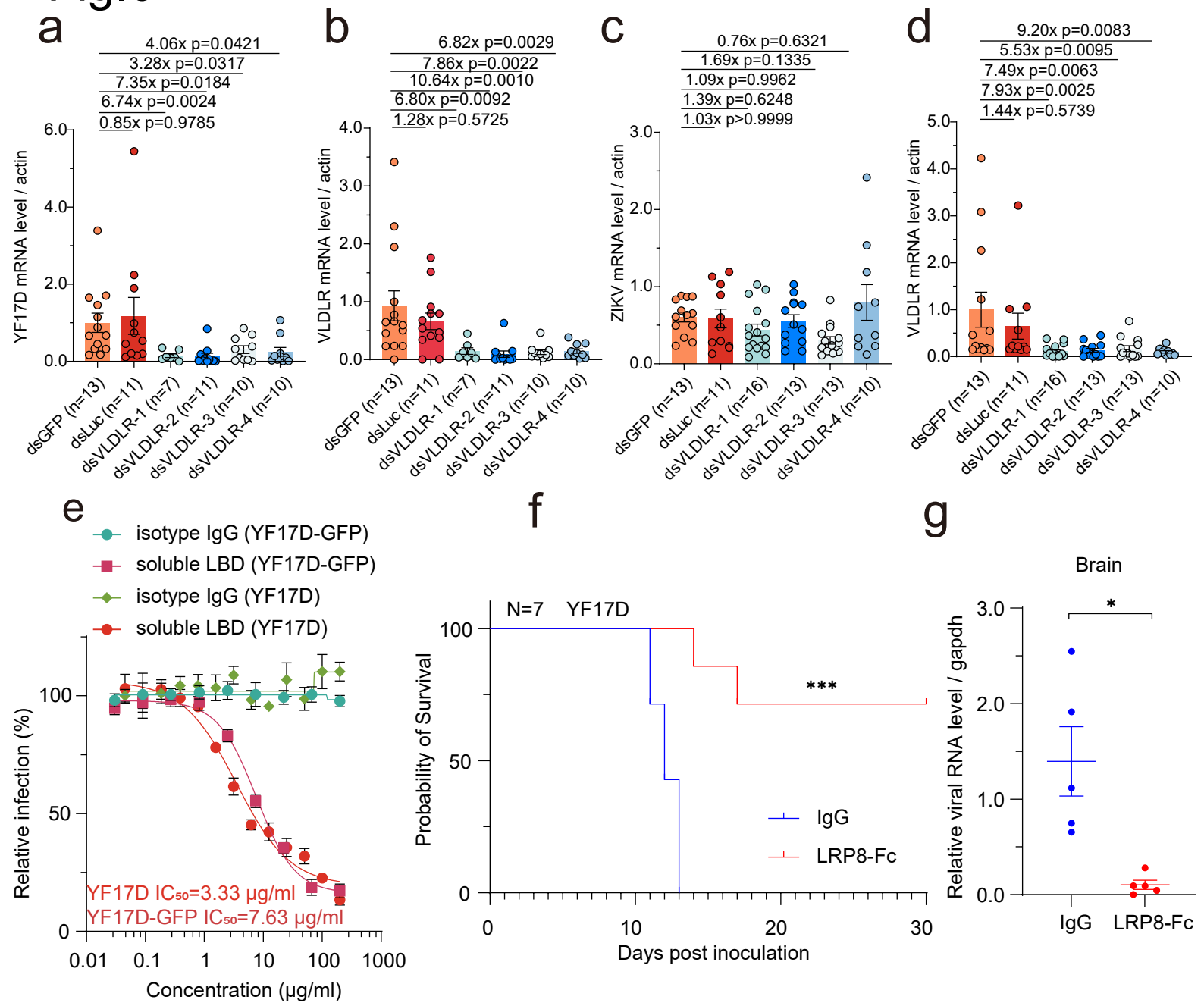
a
4.06x p=0.0421
3.28x p=0.0317
7.35x p=0.0184
6.74x p=0.0024
0.85x p=0.9785
YF17D mRNA level / actin
dsGFP (n=13)
dsLuc (n=11)
dsVLDLR-1 (n=7)
dsVLDLR-2 (n=11)
dsVLDLR-3 (n=10)
dsVLDLR-4 (n=10)
b
6.82x p=0.0029
7.86x p=0.0022
10.64x p=0.0010
6.80x p=0.0092
1.28x p=0.5725
VLDLR mRNA level / actin
c
0.76x p=0.6321
1.69x p=0.1335
1.09x p=0.9962
1.39x p=0.6248
1.03x p>0.9999
ZIKV mRNA level / actin
dsVLDLR-1 (n=16)
d
9.20x p=0.0083
5.53x p=0.0095
7.49x p=0.0063
7.93x p=0.0025
1.44x p=0.5739
VLDLR mRNA level / actin
e
isotype IgG (YF17D-GFP)
soluble LBD (YF17D-GFP)
isotype IgG (YF17D)
soluble LBD (YF17D)
Relative infection (%)
YF17D IC50=3.33 μg/ml
YF17D-GFP IC50=7.63 μg/ml
Concentration (μg/ml)
f
N=7 YF17D
Probability of Survival
***
IgG
LRP8-Fc
Days post inoculation
g
Brain
Relative viral RNA level / gapdh
*
IgG
LRP8-Fc

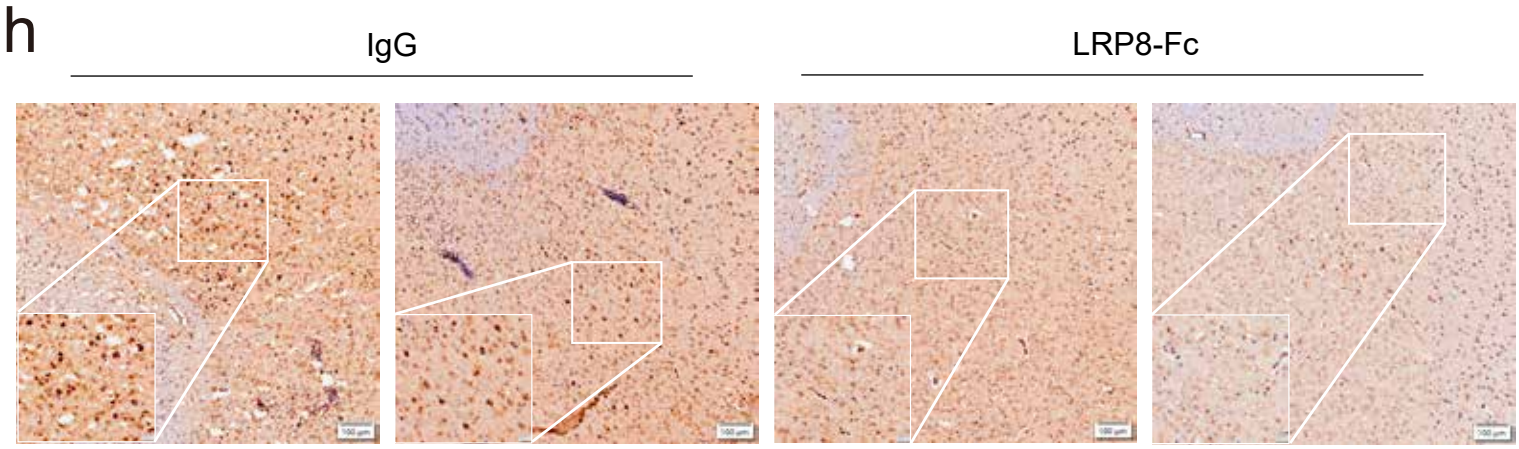
h
IgG
LRP8-Fc

Extended Figures

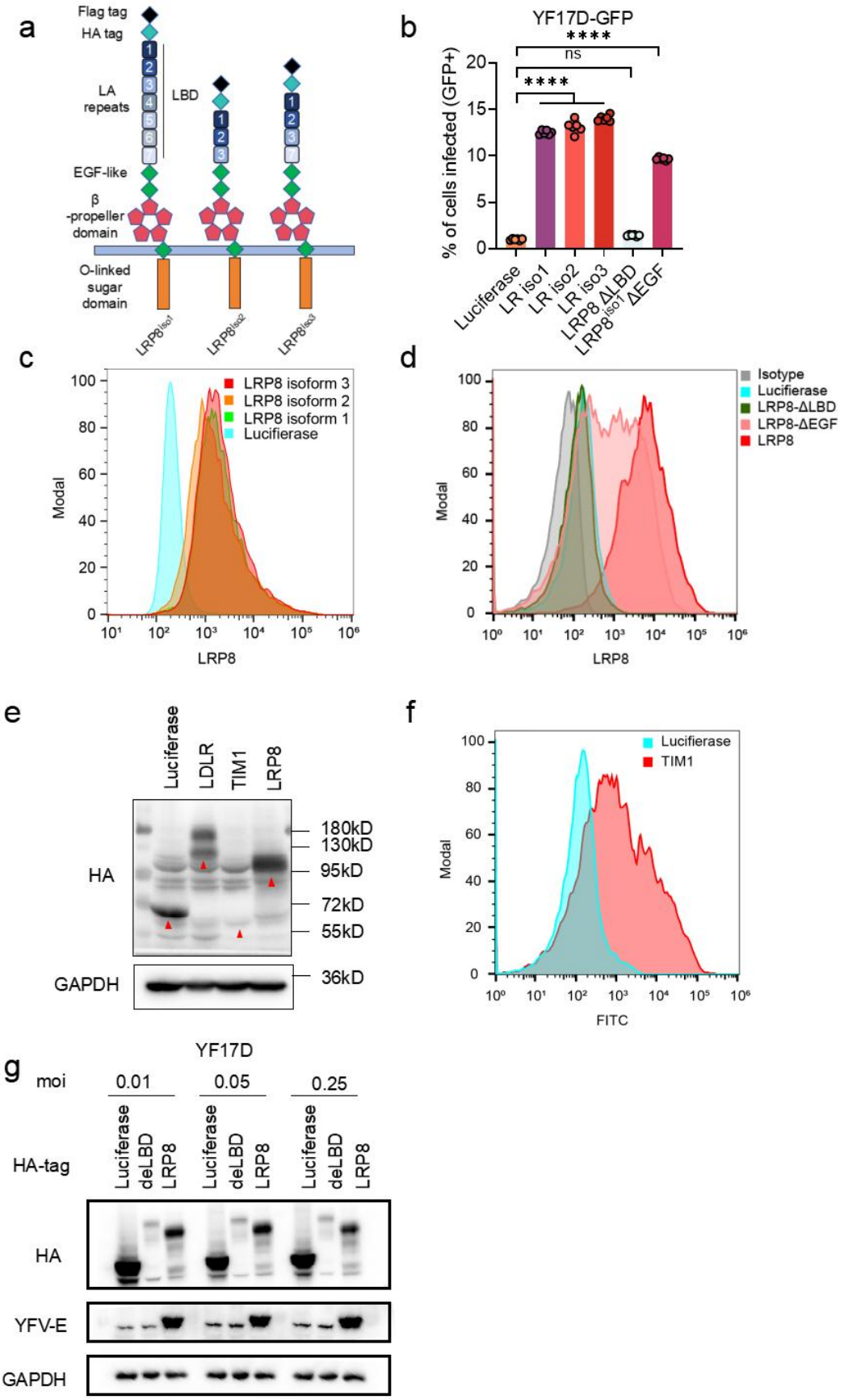

Extended Figure 1 Different major isoforms of LRP8 have similar activities in promoting YF infection. a, Schematic structure of LRP8 isoforms; **b,** In HEK293T cells, luciferase, LRP8 isoforms and its truncations were transiently overexpressed and the cells are infected by YFV 17D pseudoviruses. The ratios of infected cells were analyzed using FACS at 24hpi. **c,d,** Expression of the isoforms and its truncations on cell surface were determined with anti-LRP8 by FACS. **e, f**, Luciferase, LDLR, LRP8 or TIM1 containing 3xHA tag were analyzed by western blot in HEK293T cells or FACS. **g**. In HEK293T cells, luciferase, LRP8-ΔLBD and LRP8 were transiently overexpressed and the cells are infected by live YF17D with different MOI for 48h. The infected cells were analyzed using Western blots. Statistical analysis was performed using one-way analysis of variance (ANOVA) with Dunnett's multiple comparisons test(b). The statistics shown are Mean ± SEM. *: $P < 0.05$; **: $P < 0.01$; ***: $P < 0.001$; ****: $P < 0.0001$， ns, not significant. The replicate in the figure indicates biological replicates, the experiments were repeated at least twice.

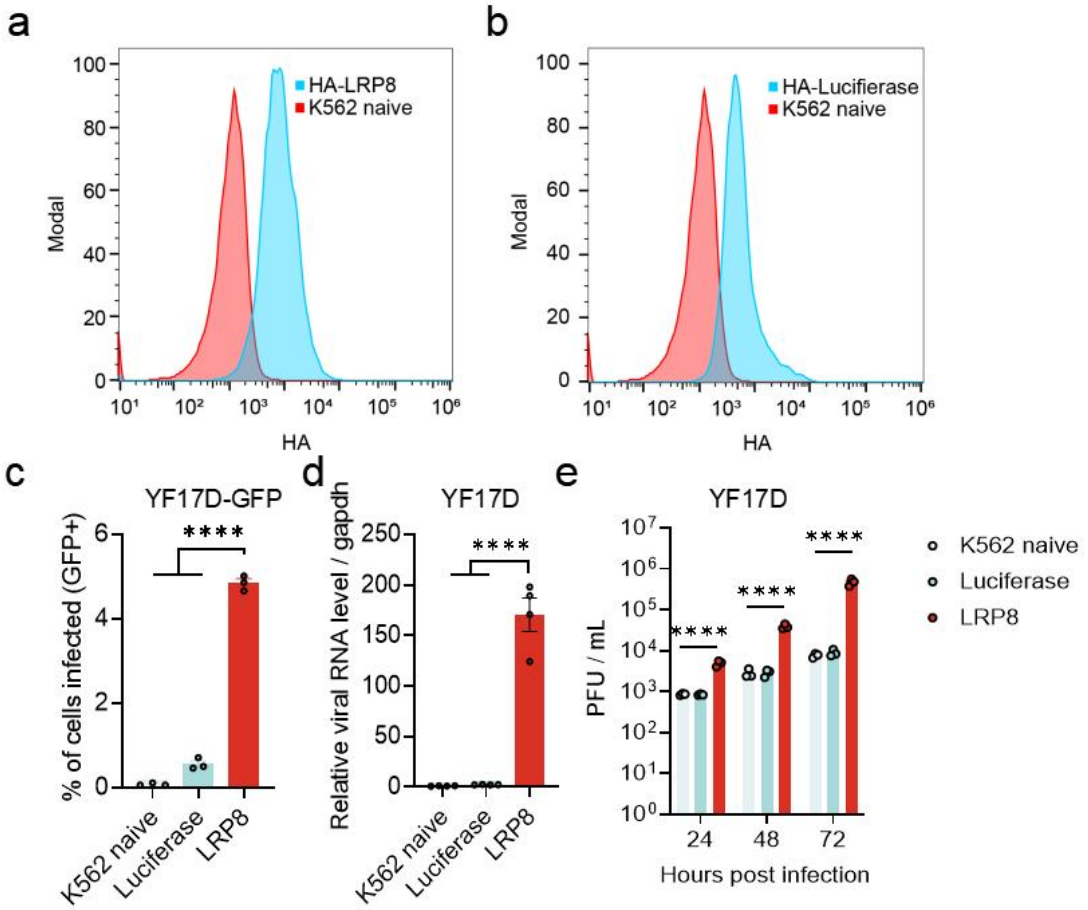

Extended Figure 2 LRP8 promotes YF17D infection in K562 cells. a, b. LRP8 and luciferase expression on K562 cell surface were determined by FACS with HA antibody staining. **c**. In K562 cells, HA-tagged luciferase and LRP8 were stably overexpressed and the cells are infected by YFV 17D pseudoviruses and the infection rates were determined by FACS at 24 hpi. **d**. In K562 cells, HA-tagged luciferase and LRP8 were stably overexpressed and the cells are infected by live YFV 17D and viral RNA level in cells were determined by qRT-PCR at 48 hpi. **e**. Infectious viral particles from d were determined by plaque assay. Statistical analysis was performed using two-way analysis of variance (ANOVA) with Dunnett’s multiple comparisons test(c-e). The statistics shown are Mean ± SEM. *: $P < 0.05$; **: $P < 0.01$; ***: $P < 0.001$; ****: $P < 0.0001$, ns, not significant. The replicate in the figure indicates biological replicates, the experiments were repeated at least twice.

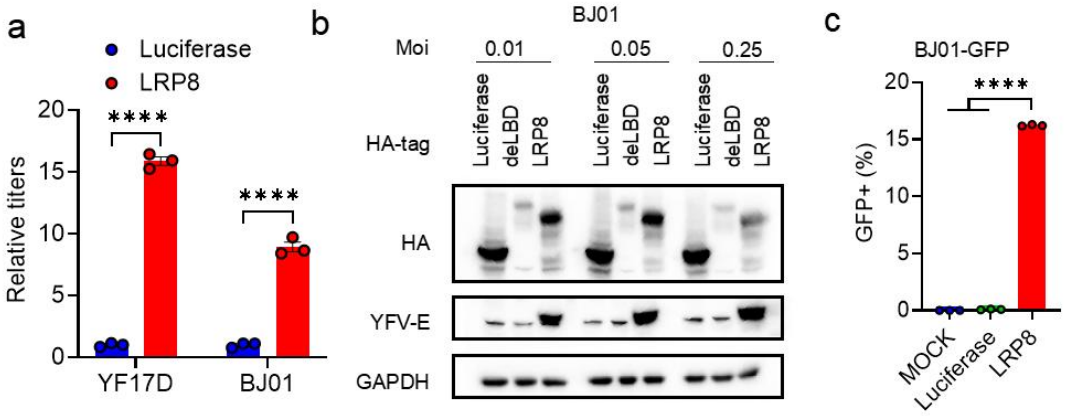

Extended Figure 3 LRP8 promotes the infection by live viruses of YF17D, BJ01 and BJ01-GFP pseudovirus. a. Supernatant of HEK293T expressing Luciferase and LRP8 infected with YF17D (0.05 MOI) and BJ01(0.05 MOI). At 48hpi, the viral titers were determined by plaque assay in BHK21 cells. **b**. In HEK293T cells, luciferase, LRP8-ΔLBD and LRP8 were transiently overexpressed and the cells are infected by live BJ01 with different MOI for 48h. The infected cells were analyzed using Western blots. **c**. In HEK293T cells, luciferase and LRP8 were transiently overexpressed and the cells are infected by YFV BJ01 pseudoviruses. The ratios of infected cells were analyzed using FACS at 24 hpi. Statistical analysis was performed using two-way analysis of variance (ANOVA) with Uncorrected Fisher's LSD test (a), Dunnett's multiple comparisons test(c). The statistics shown are Mean ± SEM. *: $P < 0.05$; **: $P < 0.01$; ***: $P < 0.001$; ****: $P < 0.0001$, ns, not significant. The replicate in the figure indicates biological replicates, the experiments were repeated at least twice.

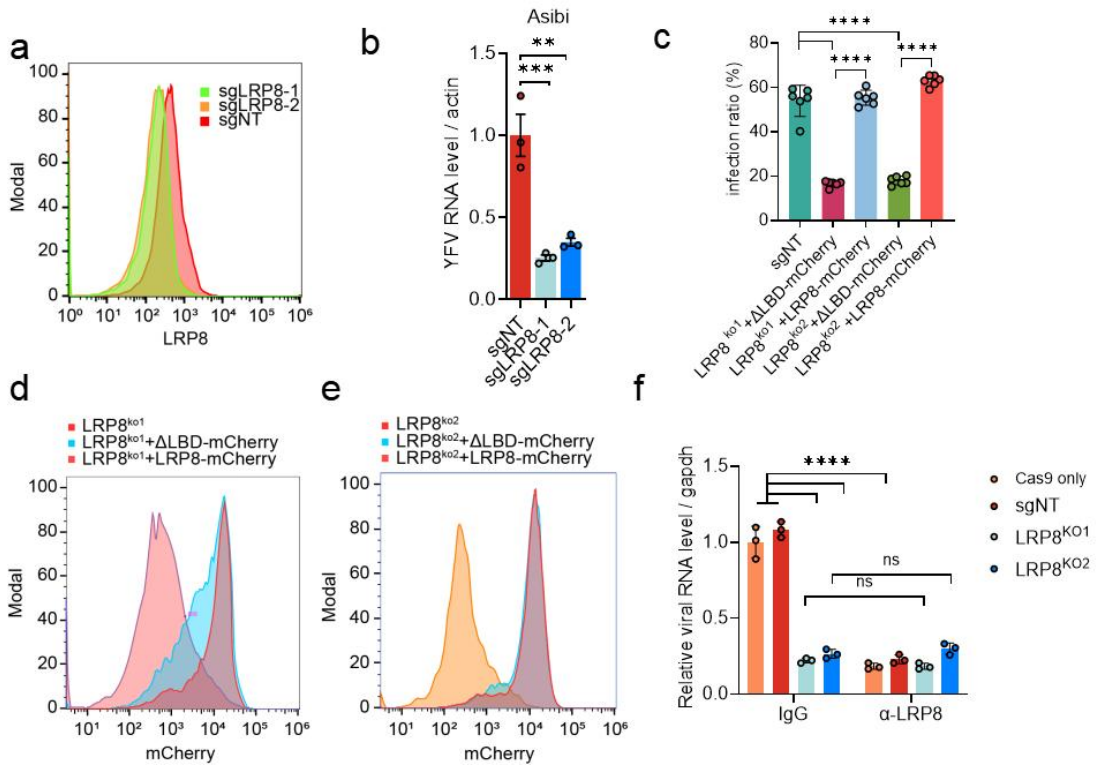

Extended Figure 4 Deficiency of LRP8 decreases live Asibi and YF17D infection. a. U87MG cells expressing Cas9/sgLRP8 single clones and Cas9 only were tested by FACS with anti-LRP8. **b**, Knockout cells were infected with the clinical Asibi (0.2 moi), viral RNA was quantified by RT–qPCR. **c-e**, In two LRP8 KO cells, ΔLBD-mCherry and LRP8-mcherry plasmids were electroporated and 48h later the cells are infected with YF17D. At 48 hpi, the cells were stained for YFV E protein and quantitated by fluorescence microscope. ΔLBD-mCherry and LRP8-mcherry expressions were determined by FACS. **f**. U87MG-sgLRP8 and control U87MG cells expressing only Cas9 were preincubated with 10 μg/ml anti-LRP8 (sc-1A1) or IgG before being infected by YF17D. At 48 hpi, the infections were analyzed by qRT-PCR. Statistical analysis was performed using two-way analysis of variance (ANOVA) with Turkey’s multiple comparisons test (b, c, f). The statistics shown are Mean ± SEM. *: $P < 0.05$; **: $P < 0.01$; ***: $P < 0.001$; ****: $P < 0.0001$，ns, not significant. The replicate in the figure indicates biological replicates, the experiments were repeated at least twice.

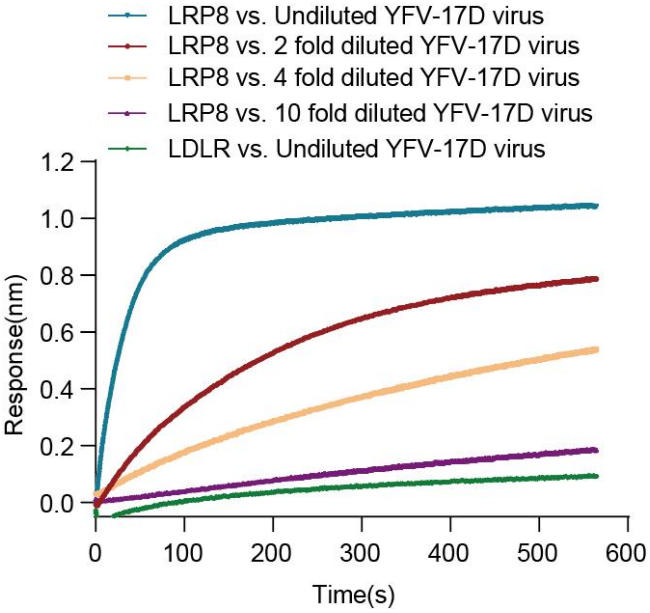

Extended Figure 5 Purified LRP8 LBD or LDLR LBD were biotinated and immobilized on the probe of biolayer inferometry (BLI). The binding of YFV 17D viral particles to LRP8 or LDLR was measured by BLI assay.

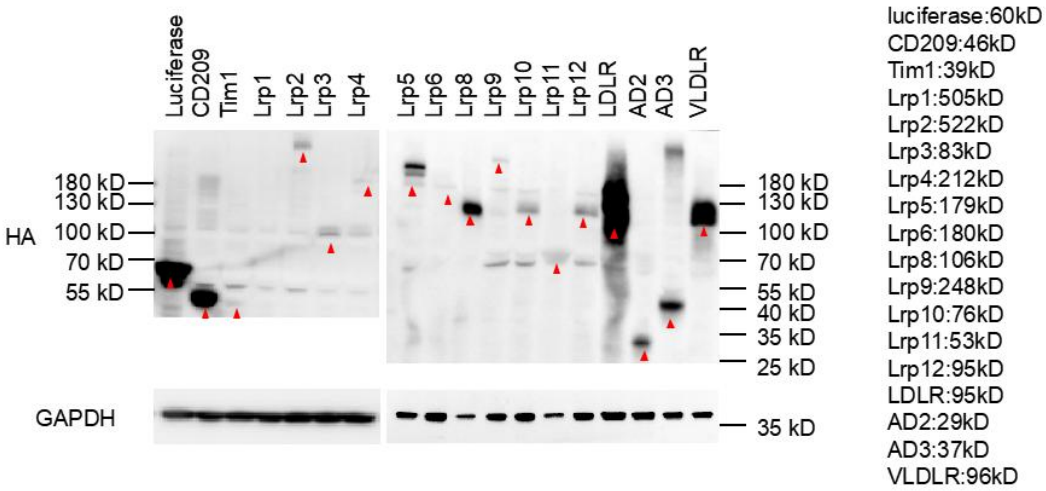

Extended Figure 6 Expression of different members of the LDLR family. In HEK293T cells, plasmids expressing different LDLR family members were transfected into HEK293T for 48 hours and the target protein containing 3X HA tag were analyzed by Western blot. The corresponding molecular weight of each protein were marked at the right of figure.

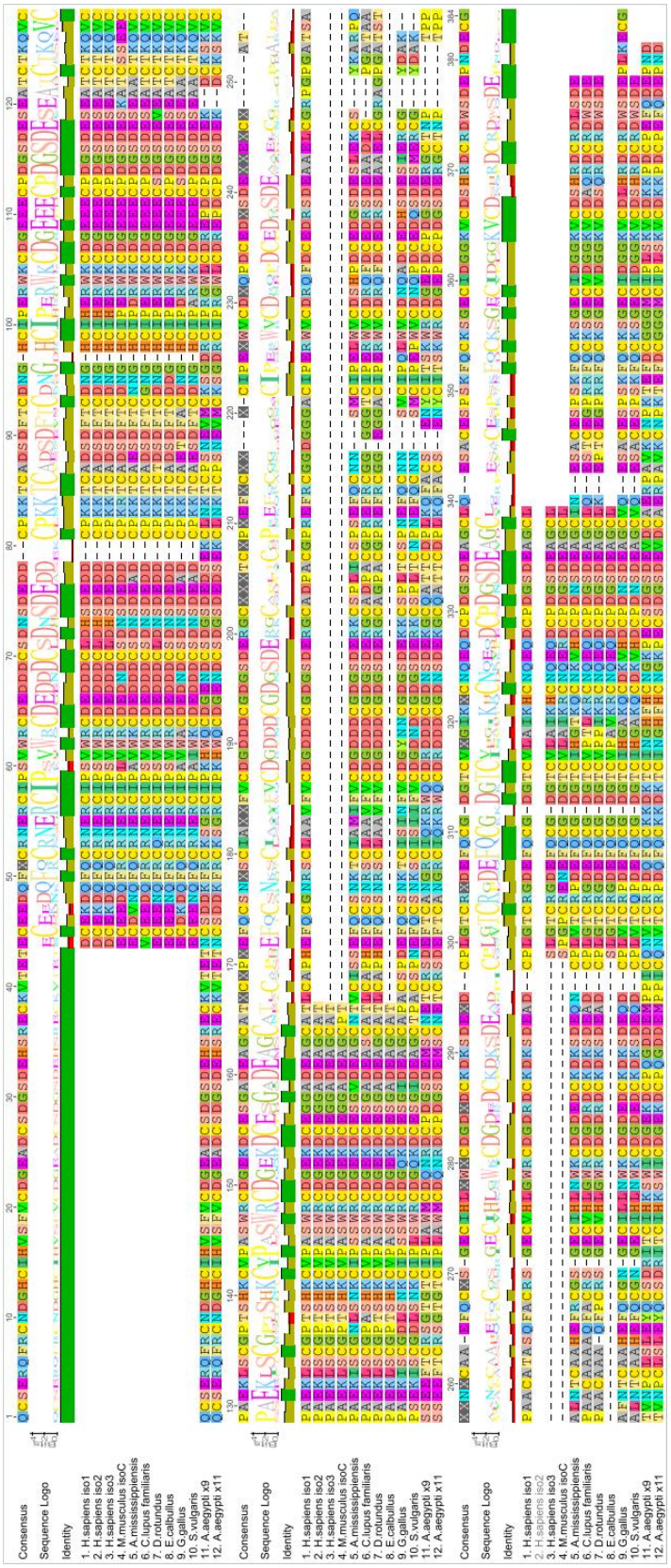

Extended Figure 7 The amino acid sequence alignment of LRP8 ligand binding domain (LBD). The LRP8 LBD amino acid sequences of human, mouse, mosquito, A. mississippiensis, bat, chicken, bird, dog, horse, green monkey were downloaded from NCBI and aligned using Geneious software.

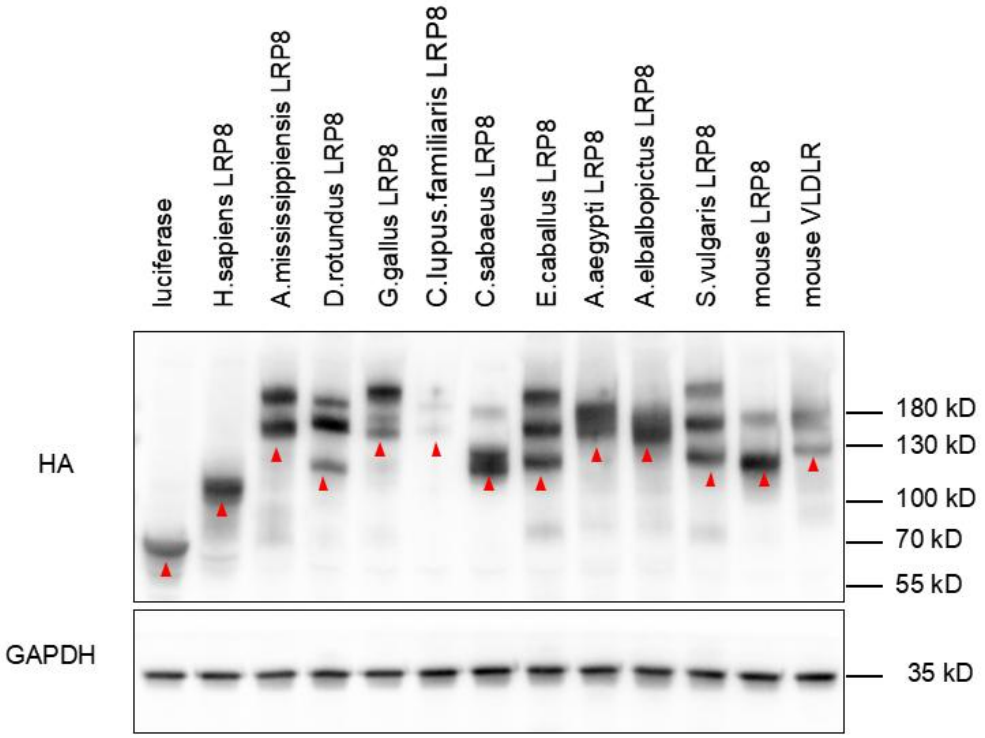

Extended Figure 8 Expression of LRP8 homologs from different species. In HEK293T cells, plasmids expressing different LRP8 orthologs were transfected into HEK293T for 48 hours and the target protein containing 3X HA tag were analyzed by Western blot.

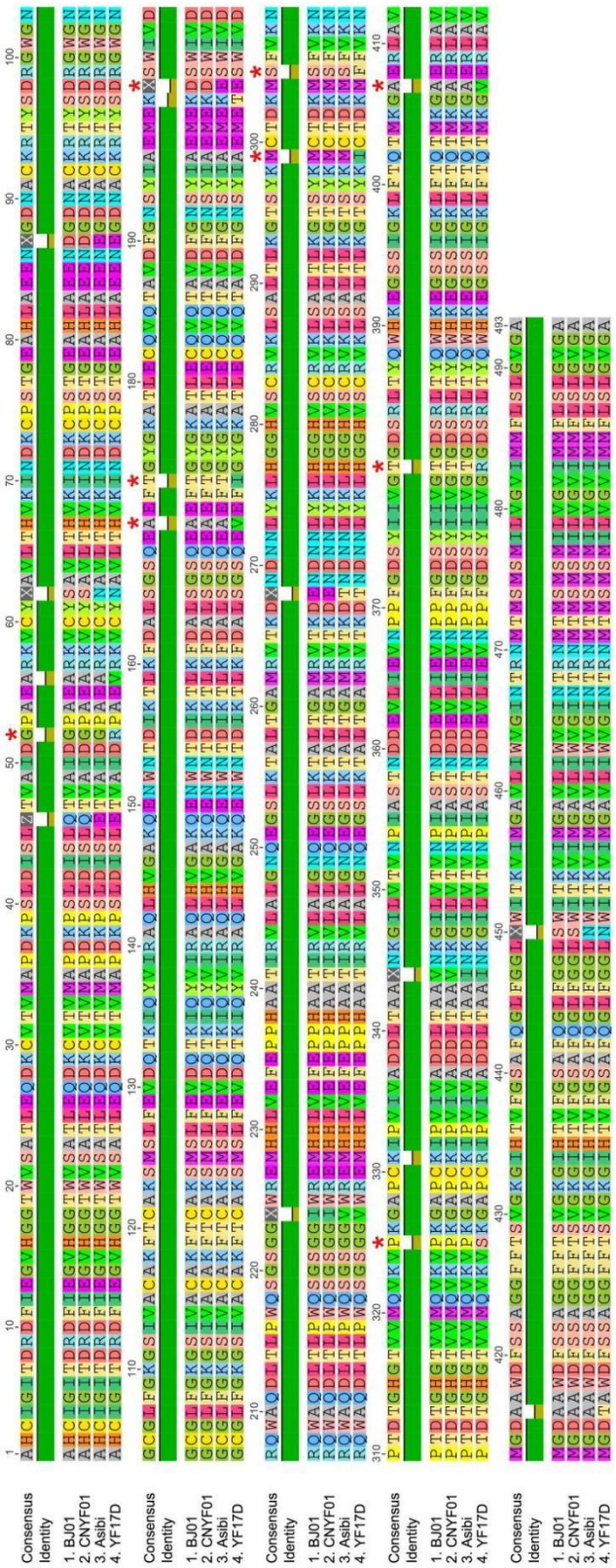

Extended Figure 9 The amino acid sequence alignment of YF strain envelope proteins. The amino acid sequence of the envelope protein of YF BJ01, CNYF01, Asibi, YF17D strains were downloaded from NCBI and aligned using Geneious software. Asterisks indicate sites of mutations in E.

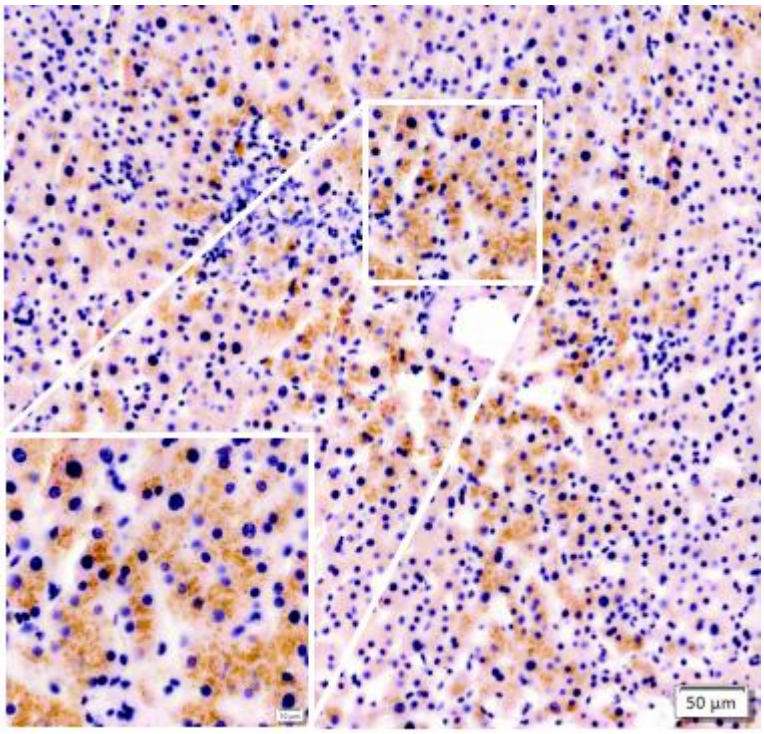

Extended Figure 10 LRP8 expression were determined in human liver sample by immunohistochemistry staining with a LRP8 antibody (Thermo 3H2 clone).

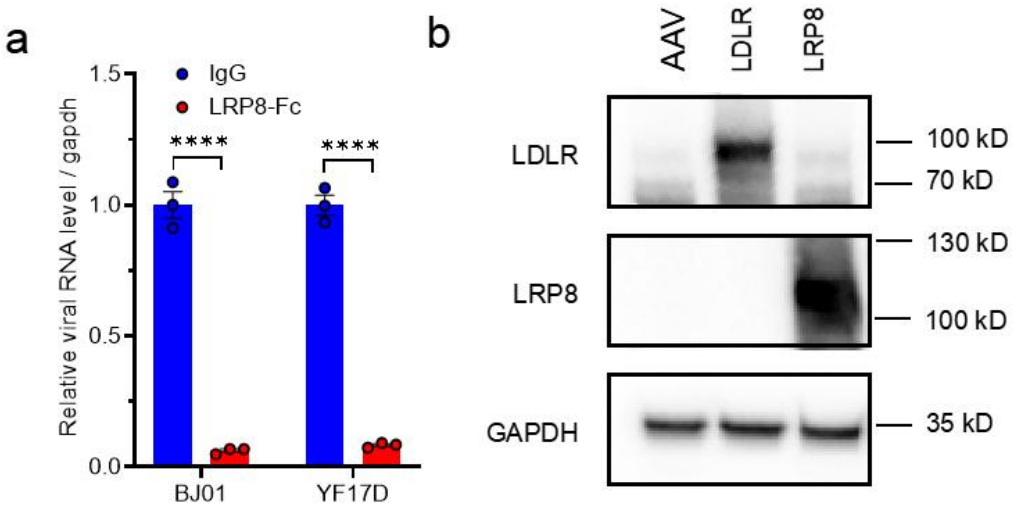

Extended Figure 11 Soluble LRP8-Fc blocks BJ01 and YF17D infection and validation of the expression of LDLR and LRP8 delivered by AAV in mouse liver. a. Preincubation of soluble LRP8 (200 μg/ml) with 0.5 MOI of BJ01 and Asibi for 1 hour, and the protein-virus mixture were added into PHHs for 48 hours. The viral RNA was quantified by qRT-PCR (three biological repeats). **b**. hLDLR and hLRP8 in mouse liver were determined at 3 weeks post AAV delivering by Western blot. Statistical analysis was performed using two-way analysis of variance (ANOVA) with Uncorrected Fisher’s LSD test (a). The statistics shown are Mean ± SEM. *: P < 0.05; **: P < 0.01; ***: P < 0.001; ****: P < 0.0001，ns, not significant. The replicate in the figure indicates biological replicates, the experiments were repeated at least twice.

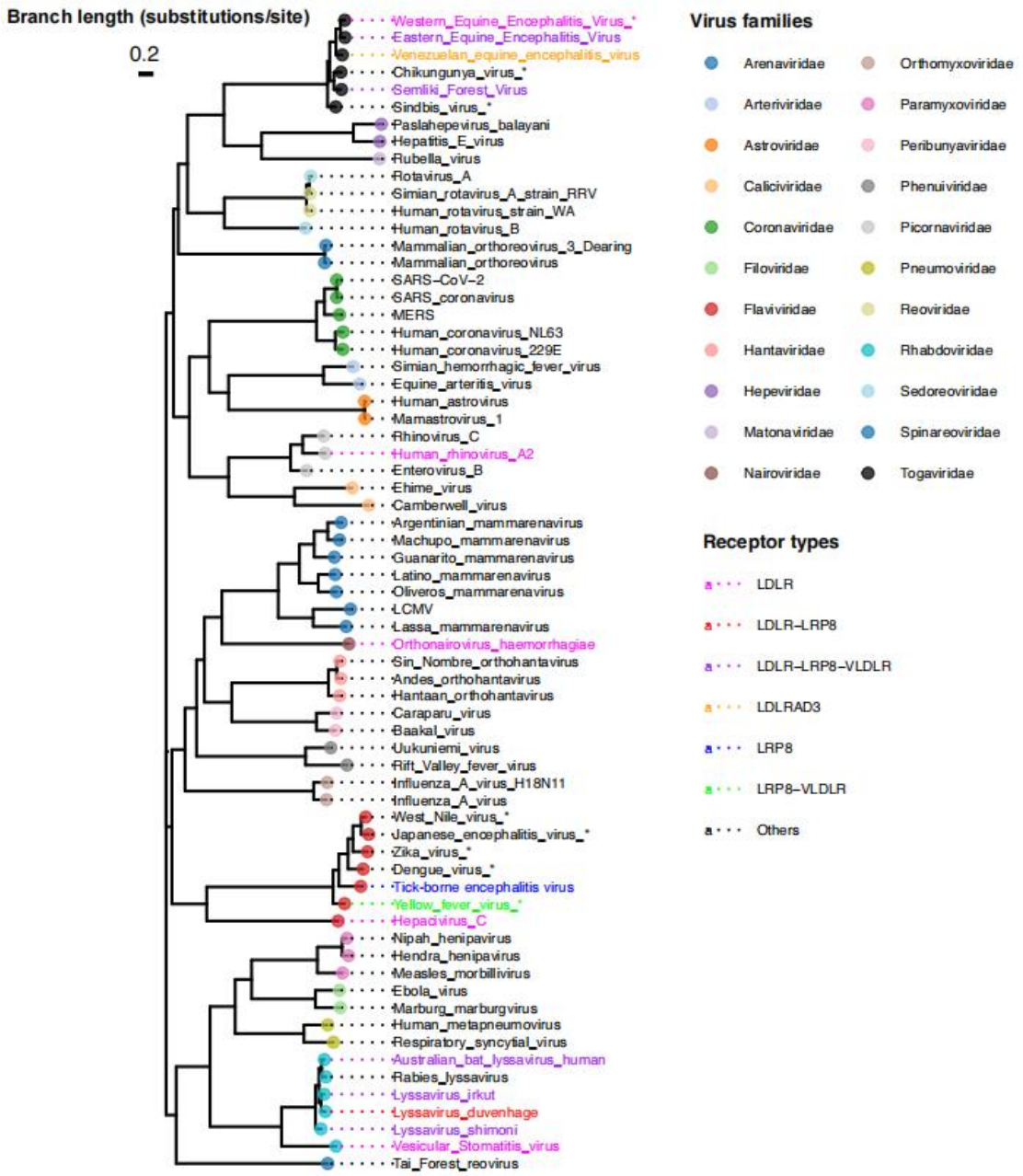

Extended Figure 12 Phylogenetic Tree Construction of RNA Virus RdRPs. To investigate the evolutionary relationships of RNA-dependent RNA polymerases (RdRPs) among human-infecting RNA viruses, we curated 24 RNA virus families from the Virus-Host Database. Receptor-annotated viruses were identified via the ViralReceptor database, covering 17 families. RdRP protein sequences were collected from NCBI, GenBank, and UniProtKB/Swiss-Prot. Among 94 viruses, all except Hepatitis delta virus, Echovirus E8, and Retroviridae had identifiable RdRPs, yielding 22 families for analysis. Sequences were aligned using MAFFT (v7.526) with the --localpair --maxiterate 1000 options, and a maximum likelihood tree was built with FastTree (v2.1.11). Visualization was done using ggtree (v3.21) in R (v4.4.3), highlighting families with known human receptors. Asterisks indicate mosquito-borne viruses.